nature communications

Article

https://doi.org/10.1038/s41467-026-68915-1

Counteracting FOX proteins epigenetically control the herpesvirus lytic-latent balance

Received: 13 August 2025

Accepted: 15 January 2026

Published online: 02 February 2026

Check for updates

Yuhang Xiang[1,2,3], Xiyuan Yang[1,2,3], Juncheng Zhang[1,2,3], Fujun Hou[1,2,3], Yue Deng[1,2,3], Hui Fu[1,2,3], Hyung Suk Oh[4], Qiongyan Wang[1,2,3], Siyu Chen[1,2,3], Zeyu Sun[1], Biswajit Das[4,5], Yao Yu Yeo[6], Jean M. Pesola[5], Pritha Sen[7,8,9,10], Sizun Jiang[6], David M. Knipe[4], Donald M. Coen[5] & Dongli Pan[1,2,3]

The lytic-latent balance is a major viral persistence strategy and obstacle to curing viral diseases, yet its mechanisms remain poorly understood. Following lytic infection in non-neuronal cells, herpes simplex virus (HSV) establishes latency specifically in neurons and is reactivated by stresses. Here we identify forkhead box (FOX) transcription factors that can strongly activate or repress replication of HSV-1 and other alphaherpesviruses, and show that neurons express activating Fox (e.g., Foxf) genes poorly but repressive Fox (Foxk) genes abundantly while non-neuronal or stressed neuronal cells exhibit higher expression of activating Fox genes. Remarkably, knockdown of Foxk1 or overexpression of activating Fox genes induces reactivation from latency in male mouse neuronal culture and in vivo. Of note, FOX proteins bind the viral genome globally and nonsequence-specifically and interact with epigenetic cofactors for gene regulation. FOXF1 interacts with CBP and P300 to acetylate and open viral chromatin. FOXK1 works with SIN3A, a cofactor of histone deacetylation, and MAX to suppress HSV-1 and antagonize activating FOX proteins. Therefore, the viral lytic-latent balance is controlled by the relative abundance of counteracting host transcription factors that recruit different epigenetic regulators to the viral genome.

Switching between productive (lytic) and latent infections is a common strategy of many viruses to persist in hosts, and a major obstacle for curing viral diseases. Herpes simplex virus 1 (HSV-1) is an ubiquitous pathogen that causes numerous human diseases. During lytic infection, after entry of the viral DNA genome into the nucleus, viral genes are expressed in the order of immediate-early (IE), early (E) and late (L) genes leading to abundant production of viral genomes and particles[1]. In vivo, after lytic infection in non-neuronal cells of peripheral tissues, HSV establishes latent infection particularly in sensory neurons where essentially all viral genes except the locus encoding the latency-associated transcript (LAT) are silenced and production of new viral genomes and particles ceases. Sporadically, certain stresses can reactivate the latent virus to resume the lytic program. HSV has evolved to strike a delicate balance between the two infection

[1]State Key Laboratory for Diagnosis and Treatment of Infectious Diseases, The First Affiliated Hospital, Zhejiang University School of Medicine, Hangzhou, Zhejiang, China. [2]Department of Microbiology, Zhejiang University School of Medicine, Hangzhou, Zhejiang, China. [3]Zhejiang Provincial Key Laboratory of Synthetic Biotechnology for Microbial Medicine, Hangzhou, Zhejiang, China. [4]Department of Microbiology, Blavatnik Institute, Harvard Medical School, Boston, MA, USA. [5]Department of Biological Chemistry and Molecular Pharmacology, Blavatnik Institute, Harvard Medical School, Boston, MA, USA. [6]Center for Virology and Vaccine Research, Beth Israel Deaconess Medical Center, Boston, MA, USA. [7]Transplant, Oncology, and Immunocompromised Host Group, Division of Infectious Diseases, Brigham and Women's Hospital, Boston, MA, USA. [8]Hematology and Oncology Group, Division of Infectious Diseases, Massachusetts General Hospital, Boston, MA, USA. [9]Department of Medicine, Harvard Medical School, Boston, MA, USA. [10]Department of Medical Oncology, Dana-Farber Cancer Institute, Boston, MA, USA. e-mail: pandongli@zju.edu.cn

programs for optimal prevalence: while lytic infection is essential for viral propagation, too much of it may cause death or evoke immune responses strong enough to clear the virus; while latency facilitates immune evasion, too deep latency may preclude spread.

Because essentially all HSV-1 proteins are used for replication, the virus relies heavily on host factors for latency, among which epigenetic factors play an important role[2,3]. During latency in vivo, the HSV-1 genome associates with histones with high levels of heterochromatin modifications such as H3K9me3 and H3K27me3[4–6], and inhibitors of the relevant histone demethylases can decrease reactivation[7–10]. PI3-K[11,12], mTOR[13] and DNA damage response[14] pathways, as well as the intrinsic and innate immunity mediated by PML nuclear body (PML-NB) components and type I interferons[15–17] are also implicated in latency. Notably, it is becoming clearer that intrinsic features of neurons favor HSV latency. The viral activator VP16 was shown to dissociate from the viral capsid in the neuronal axon so that it cannot efficiently reach the nucleus to activate gene transcription[18,19]. We showed that neuron-specific host microRNAs miR-138 and miR-9 repress the expression of multiple viral and host activators of HSV gene expression[20–23]. Regarding the mechanisms of reactivation, it has been hypothesized that stress-related JNK[24] and DLK[25] pathways lead to an initial step of viral gene de-repression before full reactivation[12]. The glucocorticoid receptor could activate lytic gene promoters in transfection assays, and its mutation reduced reactivation in female mice[26,27]. Taken together, despite the previous work revealing upstream pathways involved, little is known about what directly acts on the viral genome to enable latency specifically in neurons and reactivation under stresses.

Our previous studies showed that FOXC1, a target of miR-138, promotes HSV-1 neuronal replication[21]. FOXC1 belongs to the forkhead box (FOX) transcription factor family, which comprises 50 genes classified into 19 subfamilies in humans[28]. FOX proteins share a conserved winged helix forkhead DNA binding domain (DBD)[29]. They play pivotal roles in various biological processes including development, metabolism and oncogenesis[30–32]. Notably, the FOXA subfamily members are known as pioneer factors, which are transcription factors capable of accessing and then opening condensed chromatin[33,34]. However, the roles of FOX proteins in viral infection remain largely unexplored. For herpesviruses, we are aware of only a few related reports, which were about regulation of human cytomegalovirus (HCMV) or Kaposi's sarcoma-associated herpesvirus (KSHV) by FOXO or FOXK proteins[35–39]. Aside from our own studies regarding FOXC1[21], we are unaware of any reports on roles of FOX proteins in HSV infection.

In this work, we identified multiple FOX proteins that can strongly activate or repress neuronal replication of HSV-1 and other alphaherpesviruses. These proteins are expressed in ways that correlate with the viral phenotypes of latency or lytic replication, and perturbation of their expression profoundly impacts the lytic-latent balance in neuronal culture and in vivo. Mechanistically, the FOX proteins widely associate with viral DNA and cooperate with epigenetic regulators to modulate viral chromatin. These results lead to a new model about how the viral lytic-latent balance is controlled.

Results

Identification of FOX proteins that can strongly activate or repress HSV-1 neuronal replication

To identify FOX family proteins that can regulate HSV-1 infection, we first selected one member from each subfamily and transfected their human genes before infecting mouse neuroblastoma Neuro-2a cells (Fig. 1a, Supplementary Fig. 1a). If a *Fox* gene from a subfamily had an effect, other members of the subfamily were also tested. In case the viral E3 ubiquitin ligase ICP0 interfered with these functions[40], both wild-type (WT) strain KOS and its ICP0-null mutant (7134 virus)[41] were used. Proteins with significant impacts on both viruses at a low multiplicity of infection (MOI) were selected. Thus, FOXA1, A2, A3, C1, C2, E1, F1 and F2 that could substantially increase viral yields are designated activating FOX proteins, and FOXK1 and K2 with opposite effects are designated repressive FOX proteins (Fig. 1a). The effects were generally greater on ICP0-null than WT HSV-1 suggesting that ICP0 indeed interfered with FOX protein effects. To test whether this could be due to degradation of FOX proteins induced by ICP0, we examined FOXA1, C1, F1 and K1 expression in human embryonic kidney 293T cells infected with either WT or ICP0-null virus. Expression of these FOX proteins was similar following infection by the two viruses, with the possible exception of less FOXK1 expression in WT infected cells (Supplementary Fig. 1b), implying that instead of targeting FOX proteins for degradation, ICP0 might interfere with downstream steps regulated by the FOX proteins. To avoid such confounding interference, some mechanistic studies described below used ICP0-null virus.

For representative activating FOXF1 and repressive FOXK1, their impacts were confirmed by growth curves (Fig. 1b) and by using Neuro-2a cells stably transduced with these genes for doxycycline (DOX)-inducible expression (Fig. 1c, Supplementary Fig. 1a). Even at a high MOI, FOXK1 could also suppress both viruses, although FOXF1 could stimulate ICP0-null but not WT HSV-1 (Fig. 1d). Mouse FOXF1 and FOXK1 had the same effects as their human counterparts (Supplementary Fig. 1a, c), providing support for using mice or mouse cells to study the human proteins. The natural sites of HSV-1 infection and latency are human sensory neurons. Therefore, we employed human induced pluripotent stem cells (iPSCs)-derived sensory neurons (iNeurons)[42], and found that lentivirus transduced FOXA1, C1, E1 and F1 all substantially increased WT HSV-1 yields while FOXK1 decreased them (Fig. 1e). However, in 293T cells, transfected FOXF1 had no effect on either virus although FOXK1 decreased yields of both viruses (Fig. 1f). In human foreskin fibroblast (HFF) cells, transduced FOXF1 increased yields of ICP0-null but not WT virus while FOXK1 had no significant effect on either virus (Fig. 1g). Therefore, the effects of FOX proteins are cell-type specific but conserved in human and mouse neuronal cells.

FOX proteins can also regulate other alphaherpesviruses

To test whether similar neurotropic viruses are regulated by FOX proteins, transfection-infection experiments were conducted for some other alphaherpesviruses, including HSV-2, pseudorabies virus (PRV), and bovine herpesvirus 1 (BoHV-1) (Supplementary Fig. 2a–c). HSV-2 and PRV, but not BoHV-1, efficiently infected Neuro-2a cells. $TCID_{50}$ assays of BoHV-1 stocks in Neuro-2a cells showed slow development of cytopathic effects but $TCID_{50}$ titers similar to PFU titers in bovine kidney MDBK cells indicating efficient entry but inefficient replication. Regardless, sufficient BoHV-1 yields were obtained in Neuro-2a cells by using a high MOI (Supplementary Fig. 2c). For all three viruses, FOXF1 or K1 significantly increased or decreased viral yields, respectively (Supplementary Fig. 2a–c). We found that varicella-zoster virus (VZV) cannot infect Neuro-2a cells, but its gene expression could be detected after the genome was transfected. Co-transfecting FOXF1 with the VZV genome significantly increased *IE61* (homolog of HSV *ICP0*) and *IE62* (homolog of HSV *ICP4*) mRNA levels, while FOXK1 decreased *IE61* but not *IE62* mRNA levels (Supplementary Fig. 2d). Thus, the role of FOX proteins in regulating neuronal viral replication may be conserved in at least some alphaherpesviruses.

Fox gene expression profiles in neurons favor suppression of HSV-1

To learn about the expression patterns of *Fox* genes, we turned to RNA-seq resources including reported data for Neuro-2a, 293T[21] and Vero cells (Gene Expression Omnibus GSE182742), and the database for some other cell lines (https://www.proteinatlas.org/), as well as RNA-seq data that we generated for mock-infected human iNeurons (Fig. 2a).

https://doi.org/10.1038/s41467-026-68915-1

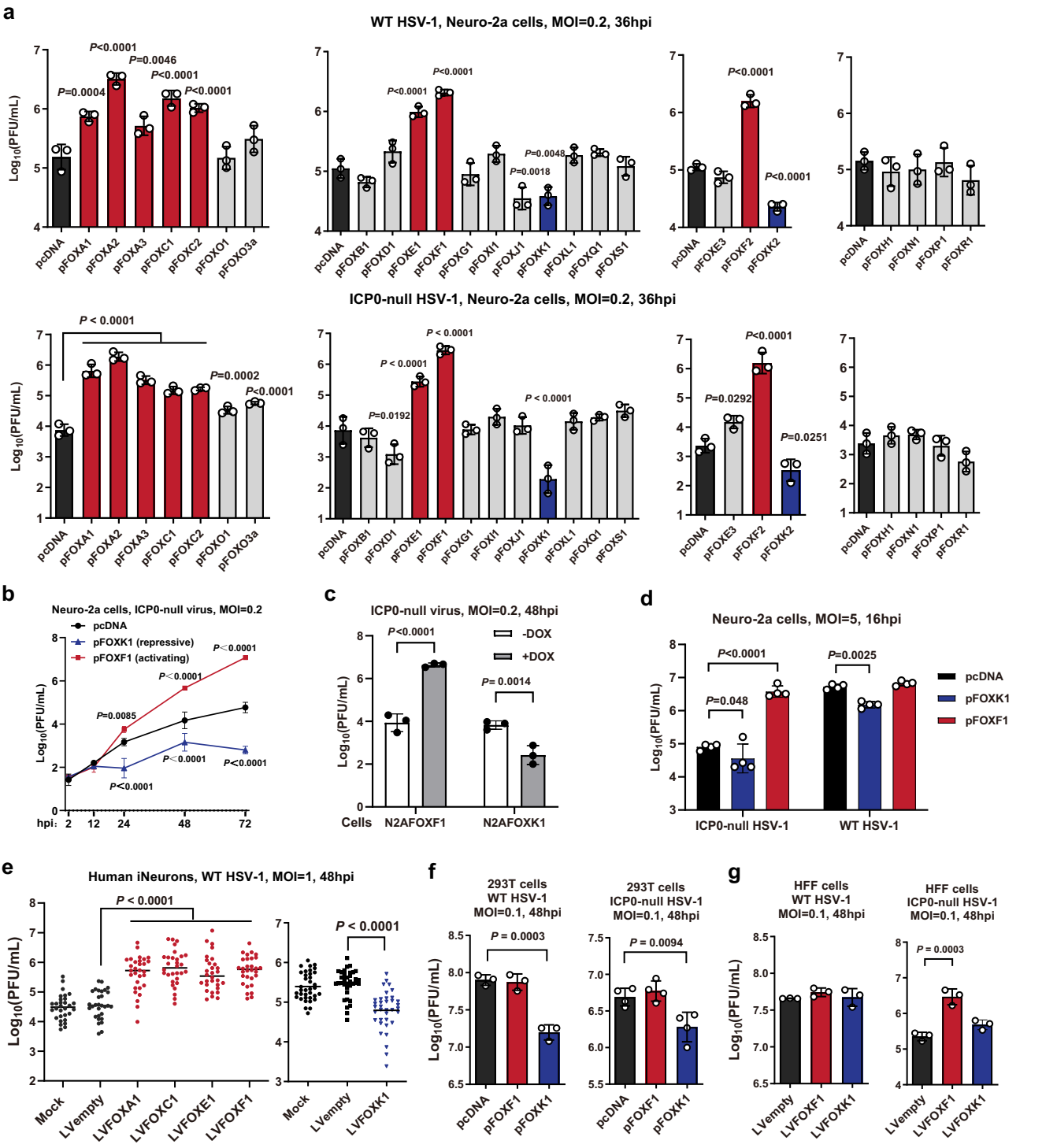


Fig. 1 | Identification of FOX proteins regulating HSV-1 replication. a Neuro-2a cells were transfected with 200 ng/mL of the indicated plasmids for 24 h, then infected with WT (upper) or ICP0-null (lower) HSV-1 before virus titration. The *P* values above each bar represent the differences with the pcDNA control. **b** After transfection and infection as in (**a**), cells were harvested at different times for virus titration. **c** N2AFOXF1 and N2AFOXK1 cells were untreated or treated with DOX for 24 h, then infected with ICP0-null virus before virus titration. **d** Same as (**a**), but with a different MOI and infection time as indicated. **e** Human iPSC-derived neurons were transduced with the indicated lentiviruses before WT HSV-1 infection and virus titration. **f** Same as (**a**) but in 293T cells. **g** HFF cells were transduced with the indicated lentiviruses, then infected with ICP0-null or WT HSV-1 before virus titration. The *P* values above the horizontal lines in (**a**) and (**e**) represent the difference between each gene under the line and the control. MOIs and infection times are specified at the top of panels. $n = 3$ (**a**–**c**, **f** left, **g**), 4 (**d**, **f** right) or 30 (**e**) biologically independent samples. Data were analyzed by one-way ANOVA with Dunnett's multiple comparisons tests (**a**, **b**, **e**, **f**, **g**) or two-way ANOVA with Sidak's multiple comparisons tests (**c**, **d**) and are presented as mean ± standard deviation (SD). Source data are provided as a Source Data file.

https://doi.org/10.1038/s41467-026-68915-1

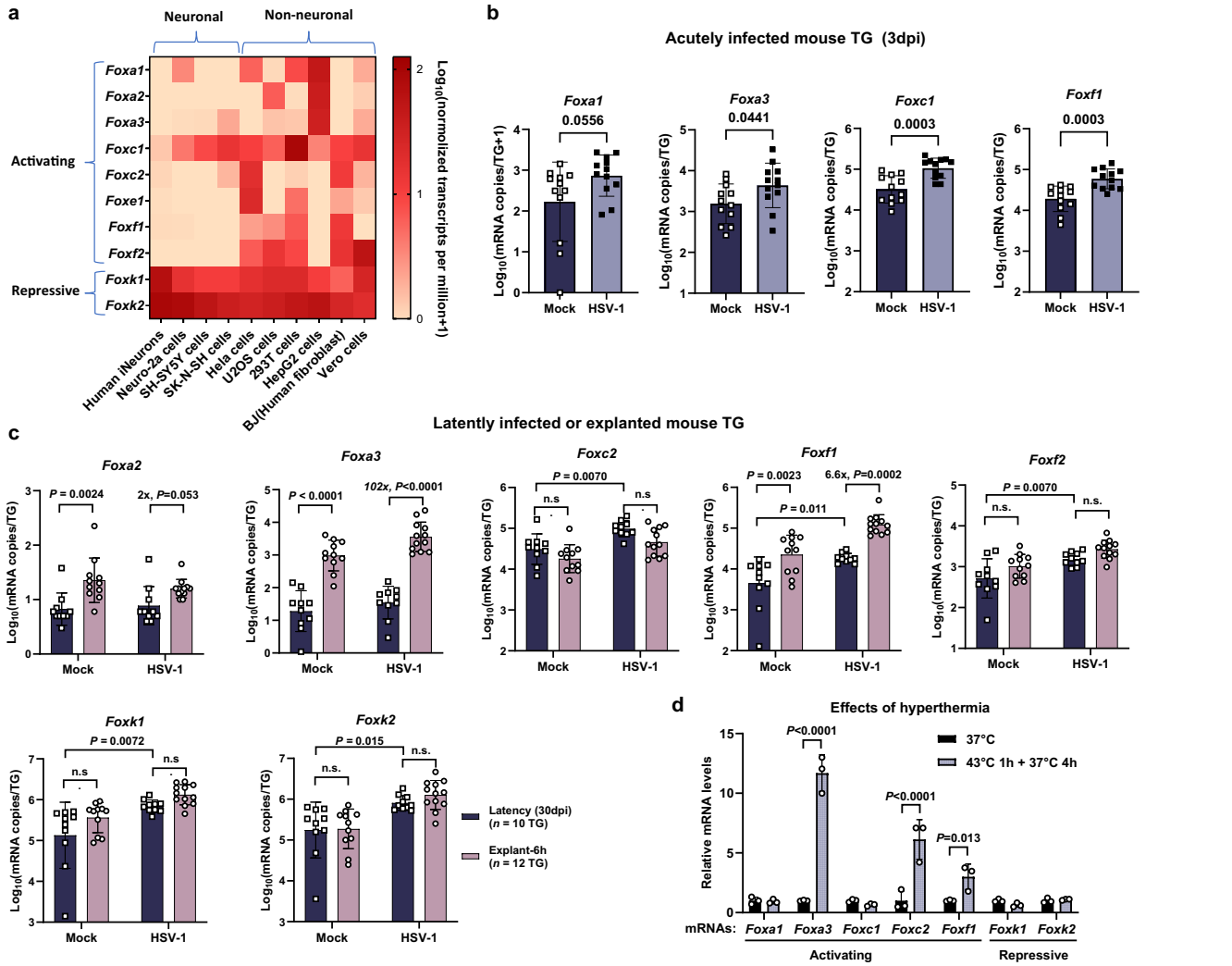


Fig. 2 | FOX gene expression patterns under different conditions. a Heatmap depicting *Fox* mRNA levels in various cells. **b** Mice were mock-infected or infected with WT HSV-1 on corneas, and TG were collected at 3 dpi for RT-qPCR analysis of the indicated mRNAs normalized to *GAPDH* mRNA. **c** Mice were mock-infected or infected with WT HSV-1 on corneas. At 30 dpi, TG were either directly collected for RT-qPCR analysis (latency samples) or explanted and cultured for 6 h before being harvested for RT-qPCR analysis (explant-6h samples). **d** Neuro-2a cells were heat-shocked at 43 °C for 1 h (or kept at 37 °C as controls), then returned to 37 °C for incubation for 4 h before being harvested for RT-qPCR analysis. $n = 3$ (**d**), 10 (**c** latency) or 12 (**b**, **c** explant) biologically independent samples. Data were analyzed by two-tailed unpaired t tests (**b**) or two-way ANOVA with Sidak's multiple comparisons tests (**c**, **d**) and are presented as mean ± SD. Source data are provided as a Source Data file.

Normalized transcript levels showed that *Foxk1* and *k2* are expressed abundantly in all cell lines examined whereas the activating *Fox* genes display differences between neuronal and non-neuronal cells. All the non-neuronal cells expressed multiple activating Fox genes abundantly with particular high expression of one or more of them. However, the neurons and neuronal cell lines all showed almost undetectable *Foxe* or *Foxf* mRNAs, and low to medium levels of certain *Foxa* or *Foxc* mRNAs. In particular, all the activating *Fox* genes were weakly expressed in iNeurons. Therefore, neuronal cells generally express activating *Fox* genes poorly but repressive *Fox* genes abundantly, which, based on our results above, should favor suppression of HSV-1.

Acute infection and stresses upregulate certain activating Fox genes

Next, we examined whether *Fox* gene expression is altered during infection or other stresses. In our RNA-seq data from HSV-1 infected iNeurons, although each experiment lacked replicates, two experiments, one with infection at MOI 1 and one at MOI 10, both hinted at upregulation of *Foxc1* (Supplementary Fig. 3a). We then infected mouse trigeminal ganglia (TG) in vivo following corneal inoculation with WT HSV-1. Relative to mock-infection, acute infection upregulated *Foxa3*, *c1* and *f1*, and possibly *Foxa1* ($P = 0.056$) at 3 days post-infection (dpi) without affecting repressive *Fox* genes (Fig. 2b, Supplementary Fig. 3b). Latent infection upregulated both activating (*Foxc2*, *f1* and *f2*) and repressive (*Foxk1* and *k2*) *Fox* genes at 30 dpi (Fig. 2c, Supplementary Fig. 3c). Explant of latently infected TG, which mimics neural damage that causes HSV-1 recurrences clinically, can trigger reactivation[43]. Relative to TG without explant, explant for only 6 h caused upregulation of *Foxa2*, *Foxa3* and *Foxf1* by ~2-, 100- and 6.6-fold, respectively, although these changes were independent of infection since mock-infected TG were affected similarly by explant (Fig. 2c, Supplementary Fig. 3c). Hyperthermia can trigger reactivation too at least in mice[44]. In Neuro-2a cells treated with hyperthermia (43°C for 1 h), *Foxa3*, *c2* and *f1* were upregulated by 12-, 6- and 3-fold, respectively (Fig. 2d). Neither explant nor hyperthermia affected *Foxk1* or *k2* mRNA levels. Thus, acute infection and reactivation-related stresses upregulate certain activating *Fox* genes without affecting repressive *Fox* genes.

https://doi.org/10.1038/s41467-026-68915-1

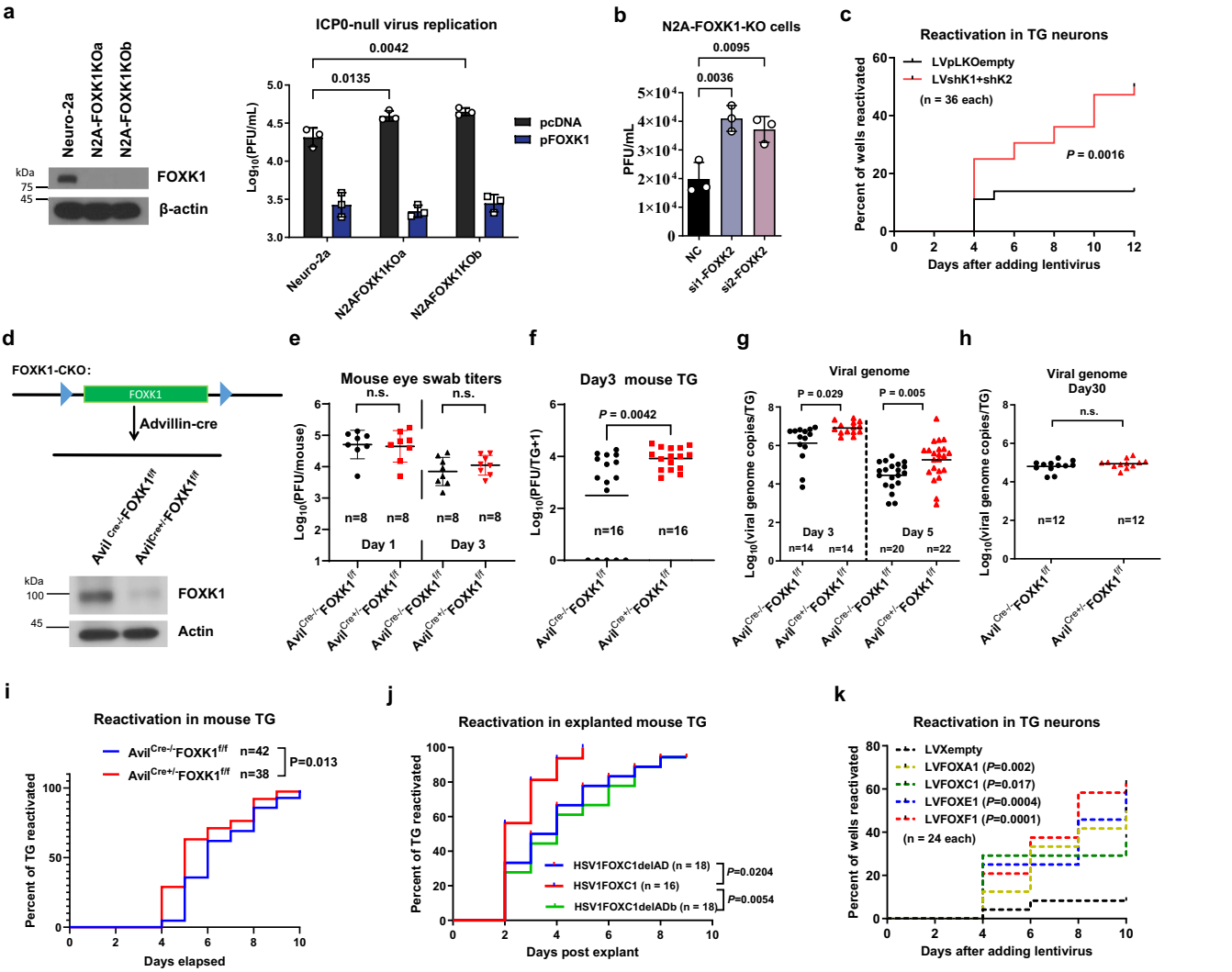


Fig. 3 | Regulation of HSV-1 neuronal replication and reactivation by FOX proteins. a Left, Western blot validation of lack of FOXK1 in the FOXK1-knockout cell lines. Right, cells were transfected with 200 ng/mL of the indicated plasmids for 24 h, then infected with ICP0-null virus (MOI = 0.2) for 48 h before virus titration. **b** N2A-FOXK1KO cells were transfected with either control or either of two FOXK2 siRNAs for 36 h, then infected with ICP0-null virus (MOI = 0.2) for 48 h before virus titration. **c** After latency was established in primary mouse TG neurons, ACV was removed and neurons were transduced with the indicated lentiviruses. Supernatants were collected for assays of infectious HSV-1. **d** Top, diagram of FOXK1 conditional knockout in mice. Bottom, mouse TG were lysed for Western blot analysis. This experiment was repeated twice with similar results. **e**–**i** The indicated mice were ocularly inoculated with 2×10^6 PFU/eye of WT HSV-1. Viral titers in eye swabs (**e**) or TG (**f**) were determined. Viral genomes were quantified by qPCR at different times (**g**, **h**). At 30 dpi, TG were explanted and reactivation rates were determined by assaying for infectious virus positivity at different times (**i**). **j** WT ICR mice were ocularly infected with 2×10^5 PFU/eye of the indicated viruses before reactivation analysis as in (**i**). **k** Reactivation analysis in primary mouse TG neurons as in (**c**). $n = 3$ (**a**, **b**) biologically independent samples. For other panels, the labeled n values represent numbers of mice (**e**), TG (**f**, **j**) or wells (**c**, **k**). Data were analyzed by one-way ANOVA with Dunnett's multiple comparisons tests (**b**), two-way ANOVA with Sidak's multiple comparisons tests (**a**, **e**, **g**), pairwise log-rank (Mantel-Cox) tests (**c**, **i**, **j**, **k**) or two-tailed unpaired t tests (**f**, **h**), and are presented as mean ± SD. Source data are provided as a Source Data file.

FOXK1 suppresses lytic replication and is important for HSV-1 latency

Given their abundance, we examined the role of endogenous FOXK proteins. Knockout (KO) of FOXK1 in Neuro-2a cells increased ICP0-null virus yields, which were reduced again by transfected FOXK1 (Fig. 3a). In the FOXK1 KO cells, siRNAs that effectively knocked down FOXK2 (Supplementary Table 1) increased viral yields further (Fig. 3b). We then employed a mouse primary TG neuron model of latency and reactivation, which usually relies on chemical triggers to induce reactivation[23]. Considering possible functional redundancy between FOXK1 and K2, we attempted dual knockdown. We selected one shRNA for FOXK1 and one for FOXK2 that effectively knocked down the respective proteins (Supplementary Fig. 1a). Remarkably, even without chemical triggers, dual knockdown of FOXK1 and K2 caused reactivation from latency in 50% of the wells, significantly higher than the 14% of control wells reactivated (Fig. 3c).

To examine the role of FOXK1 in vivo, we generated FOXK1$^{f/f}$ mice with LoxP sites flanking the *Foxk1* gene and crossed them with Advillin-Cre (Avil$^{Cre+/-}$) mice which express *Cre* specifically in sensory neurons[45]. The resulting FOXK1-conditional knockout (cKO) (Avil$^{Cre+/-}$Foxk1$^{f/f}$) mice expressed less FOXK1 in TG than the control Avil$^{Cre-/-}$Foxk1$^{f/f}$ mice (Fig. 3d). After corneal inoculation, viral titers in tear films from FOXK1-cKO mice were not different from those in control mice at 1 and 3 dpi (Fig. 3e) but were significantly higher in TG at 3 dpi (Fig. 3f) consistent with FOXK1 specifically repressing HSV-1 replication in sensory neurons. Accordingly, viral genome levels in FOXK1-cKO mice were also higher at 3 and 5 dpi (Fig. 3g). However, latent viral genome levels at 30 dpi were essentially identical between FOXK1-cKO and control mice

(Fig. 3h). Nevertheless, following explant, the virus reactivated from latently infected TG of FOXK1-cKO mice faster than those of control mice (Fig. 3i). Therefore, FOXK1 not only suppresses acute viral replication to expedite latency establishment, but is also important for latency maintenance.

Activating Fox proteins are sufficient to stimulate reactivation from latency

To investigate the effects of activating FOX proteins on latency, we first utilized previously constructed a recombinant HSV-1 expressing FOXC1 (HSV1FOXC1) and, as controls, two viruses, each of which expresses an inactive FOXC1 mutant with both N-terminal and C-terminal activating domains of FOXC1 deleted (HSV1FOXC1delAD and HSV1FOXC1delADb). In our previous study, HSV1FOXC1 exhibited increased acute titers and similar latent viral loads in mouse TG relative to the control viruses, but reactivation was not tested[21]. Here we found that after corneal inoculation and latent infection of mice in vivo, HSV1FOXC1 reactivated significantly faster than both control viruses during explant of the latently infected TG (Fig. 3j). We then employed the mouse neuronal model of HSV-1 latency mentioned above, and found that even without chemical inducers, transduced Foxa1, c1, e1 and f1 could all lead to 40–60% of wells reactivated, significantly higher than the <10% of control wells reactivated (Fig. 3k). Therefore, increased expression of activating *Fox* genes is sufficient to trigger reactivation from latency.

Widespread occupancy of FOXF1 on the HSV-1 genome

To understand how FOX proteins regulate HSV-1 infection, we first asked whether these proteins associate with viral DNA. The following studies focused mainly on FOXF1 and FOXK1 as examples of an activator and repressor, respectively, of viral replication and reactivation. We first performed chromatin immunoprecipitation (ChIP)-qPCR using an anti-FOXF1 antibody to analyze DNA association in HSV-1-infected 293T cells, where endogenous FOXF1 is abundant (Fig. 4a). As positive controls, regions in host *Gpr20* and *Kit* gene enhancers, which are known to associate with FOXF1[46], were significantly enriched in DNA precipitated by the FOXF1 antibody relative to the negative control IgG. For both WT and ICP0-null viruses, FOXF1 associated strongly not only with regions within viral *UL22* and *UL50* genes that contain the DNA motif for FOXF1 association [46], but also with *ICP8* and *ICP27* promoters that contain no such sequence. An antibody against FOXP1, which does not regulate HSV-1 (Fig. 1a), also precipitated DNA enriched with these regions implying that DNA association is insufficient to confer gene regulation. Additionally, we observed that some FOXC1 co-localized with viral replication compartments (Supplementary Fig. 4a), also consistent with association of FOX proteins with viral DNA.

To investigate this in neuronal cells, where FOXF1 is poorly expressed, we conducted ChIP-seq by pulling down transfected FOXF1 in Neuro-2a cells infected with ICP0-null virus. The positions of viral and host peaks and their corresponding genes are listed in Supplementary Data 1. Validating the results, many host peaks are positioned on FOXF1 target sites reported previously in a database (Data source: Cistrome Data Browser, GSM2062274) and a published report[46], including those within *Etv1*, *Gpr20*, *Fos*, *Sfi1* and *Bcl10* genes. Regarding the viral genome, the data reveal widespread occupancies of FOXF1 on numerous sites that were highly consistent between two biological replicates (Fig. 4b). The fraction of viral reads in total reads was 16-fold higher in the immunoprecipitated samples than input samples further indicating high enrichment of viral DNA associated with FOXF1 (Fig. 4c). The viral peaks showed little or no enrichment around transcription start sites (TSS), contrasting with clear enrichment of host peaks at TSS (Supplementary Fig. 4b) indicating differential occupancy patterns between viral and host DNA. Motif search identified the known DNA motif for FOXF1 as well as some de novo motifs that all conform to a RTAAACA sequence (R = purine) (Fig. 4c). Indeed, all RTAAACA sequences in the viral genome have peaks associated with them. However, many other viral sequences also show peaks despite lacking this consensus sequence, and ChIP-qPCR results showed that besides associating with the sites containing RTAAACA (motif$^+$ sites) in the *UL2*, *UL22* and *UL55* genes, FOXF1 also associated with the *ICP27* and *ICP8* promoters lacking RTAAACA (motif$^-$ sites) (Fig. 4d). Thus, FOXF1 extensively associates with the HSV-1 genome in both sequence-specific and nonsequence-specific (non-specific) manners.

Non-specific DNA interactions are crucial for HSV-1 regulation by FOX proteins

We also performed ChIP-qPCR for repressive FOXK1 and found robust association with the same set of viral sites as for FOXF1 above (Fig. 4e). FOX proteins comprise well-defined DBDs as well as other domains that are well-defined for FOXA and C proteins but less so for FOXE, F or K proteins[30] (Supplementary Fig. 5a, b). By using plasmids expressing truncated proteins (Supplementary Fig. 5c, d), we found that HSV-1 stimulation by FOXF1 required its DBD and the region between aa200–300 (Supplementary Fig. 5e) while efficient suppression by FOXK1 required its DBD, the C-terminus and possibly N-terminus (Supplementary Fig. 5f) suggesting that the DBDs were necessary but insufficient for virus regulation. We further constructed plasmids expressing proteins with the DBD of FOXC1 replaced with that of FOXA1, E1, F1 or K1 (Supplementary Fig. 5c, d). Remarkably, the chimeric proteins, even including the one with the DBD of repressive FOXK1, could all strongly stimulate viral replication (Fig. 4f) indicating that DBDs of different FOX proteins function similarly but are insufficient to determine activation or repression. Based on a crystal structure, the FOXC2 DBD contacts DNA mainly through an asparagine-histidine (NH) site that interacts with DNA bases, and arginine-arginine (RR) and serine-tryptophan (SW) sites that interact with DNA backbones[47] (Fig. 4g). Surprisingly, mutating the corresponding NH site in FOXC1 had no effect on virus stimulation, mutating the RR site had partial effects, while mutating both residues or just the tryptophan of the SW site eliminated stimulation (Supplementary Fig. 5g). Similar mutagenesis studies of FOXF1 showed that among the three sites, only the corresponding tryptophan in the HW site (the serine in the FOXC SW site becomes histidine in FOXF1) is essential for stimulation (Fig. 4h). Moreover, substitution of this tryptophan eliminated virus stimulation by FOXA2 and E1 and attenuated suppression by FOXK1 (Fig. 4i, j, Supplementary Fig. 5d). The substitution also greatly reduced the association of FOXF1 with the HSV-1 promoters (Fig. 4k). Therefore, non-specific DNA backbone interactions, mediated by the conserved tryptophan, are critical for HSV-1 regulation by FOX proteins.

FOXF1 can activate HSV-1 genes and modulate HSV-1 chromatin globally at early times post-infection

We next investigated which viral genes were regulated by FOX proteins and at what stage. At both 3 and 6 hpi with ICP0-null HSV-1, transfected FOXF1 and FOXK1 did not affect viral DNA levels (Fig. 5a), but significantly increased and decreased, respectively, *ICP27* (IE gene), *TK* (E gene) and *gC* (L gene) mRNA levels regardless of the presence of ACV (Fig. 5b) demonstrating that FOX proteins regulate viral gene transcription at an early stage independent of DNA synthesis.

Regulation of gene transcription is often related to chromatin remodeling. Therefore, we analyzed the association of viral DNA with histone H3 and its modifications by ChIP-qPCR. The occupancies of repressive H3K9me3 and activating H3K18ac and H3K27ac were normalized to those of H3 to assess the fractions of H3 that were modified. Both motif$^-$ and motif$^+$ sites were examined. At 2 hpi in N2AFOXF1 cells, DOX-induced FOXF1 expression already significantly decreased total H3 on most sites (Supplementary Fig. 6a, left panel) and decreased H3K9me3/H3 on the *ICP8* site while increasing H3K18ac/H3 and

https://doi.org/10.1038/s41467-026-68915-1

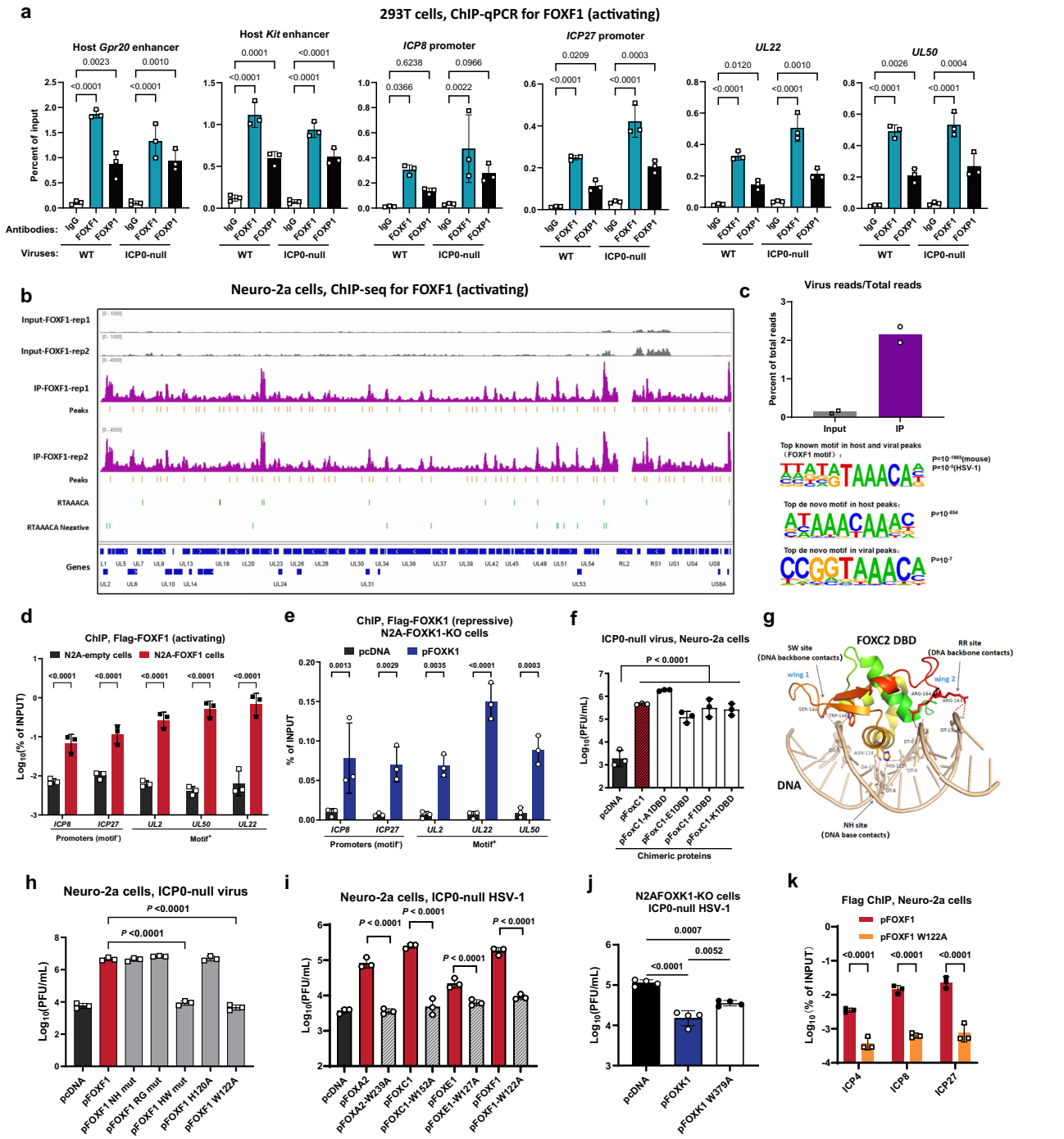


Fig. 4 | Association of FOX proteins with the HSV-1 genome. a 293T cells were infected with WT or ICP0-null HSV-1 (MOI = 10) for 5 h before ChIP-qPCR analysis using an FOXF1 or FOXP1 antibody or an IgG control. **b** Neuro-2a cells were transfected with pFOXF1 (Flag-tagged) for 42 h, then infected (MOI = 5) for 5 h before ChIP-seq analysis using an anti-Flag antibody. Shown are coverage plots for reads aligned to the HSV-1 genome with terminal repeat regions deleted. Orange vertical sticks represent peaks. Green vertical sticks represent positions of RTAAACA or its complementary sequence. **c** Upper: the percentages of viral reads relative to total reads in the ChIP-seq data. Lower: Motif analysis of the ChIP-seq data. **d** N2AFOXF1 and N2Aempty cells were treated with DOX for 42 h, then infected (MOI = 5) for 5 h before ChIP-qPCR analysis of the indicated sites using an anti-Flag antibody. **e** N2A-FOXK1KO cells were transfected with pFOXK1 for 42 h, then infected (MOI = 5) for 5 h before ChIP-qPCR analysis as in (**d**). **f** Neuro-2a cells were transfected with 200 ng/mL of the indicated plasmids for 24 h before infection and virus titration. The *P* value represents the difference between each gene under the horizontal line and the control. **g** The crystal structure of the FOXC2 DBD with DNA was visualized using PyMOL software (PDB ID: 6AKO), with key interactions highlighted. **h**–**j** Transfection-infection experiments in Neuro-2a (**h**, **i**) or N2A-FOXK1KO cells (**j**) performed as in (**f**). **k** ChIP-qPCR analysis performed as in (**d**). All infections used ICP0-null HSV-1. Cells were infected (MOI = 0.2) for 48 h for (**f**, **h**, **i**, and **j**). $n = 2$ (**b**, **c**), 3 (**a**, **d**, **e**, **f**, **h**, **i**, **k**) or 4 (**j**) biologically independent samples. Data were analyzed by one-way ANOVA with Dunnett's multiple comparisons tests (**a**, **f**, **h**, **i**, **j**) or two-way ANOVA with Sidak's multiple comparisons tests (**d**, **e**, **k**) and are presented as mean ± SD. Source data are provided as a Source Data file.

https://doi.org/10.1038/s41467-026-68915-1

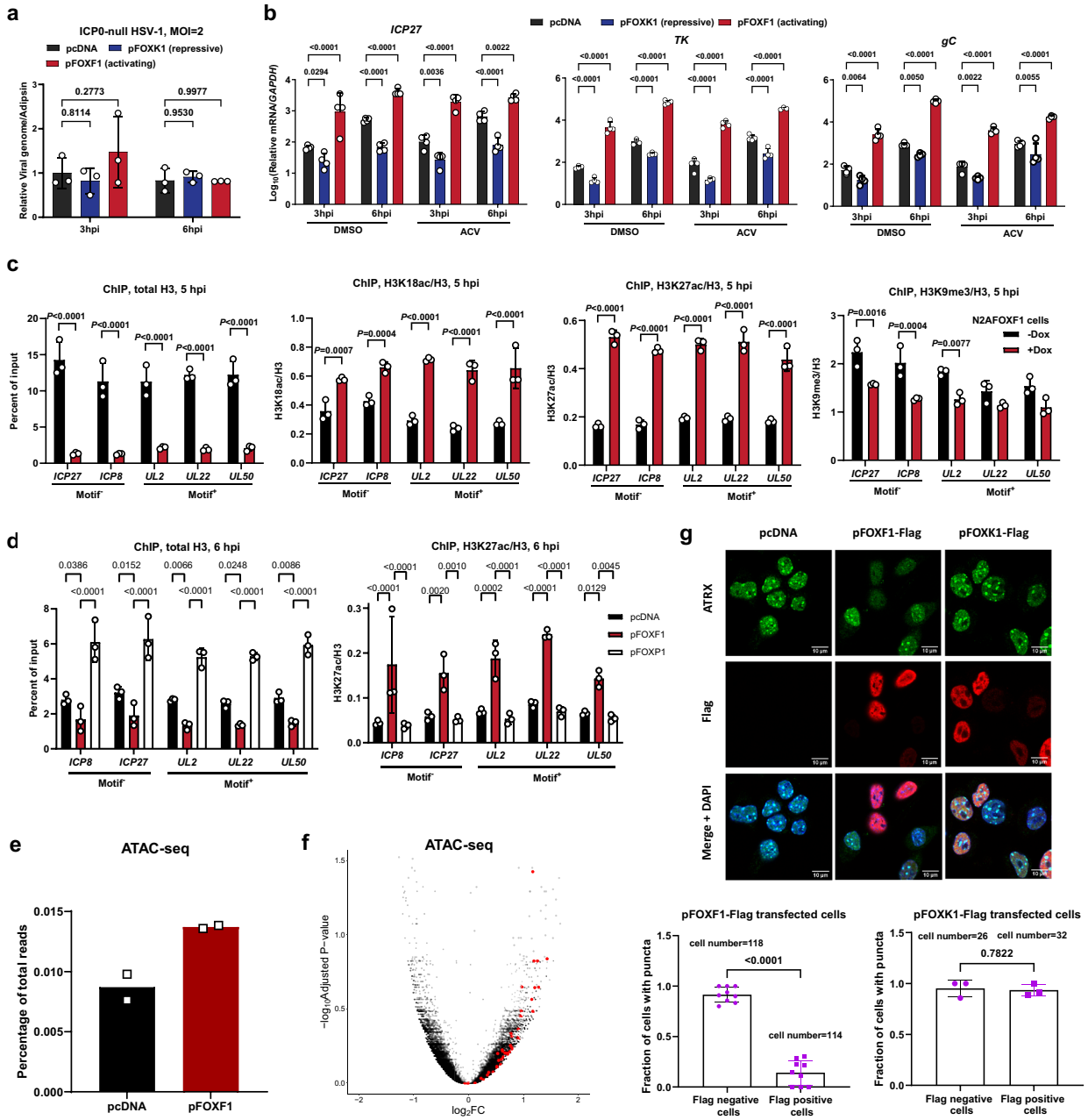


Fig. 5 | FOXF1 can activate viral genes and chromatin. a, **b** Neuro-2a cells were transfected with 200 ng/mL of the indicated plasmids for 24 h, then infected (MOI = 2) for the indicated times before qPCR analysis of viral genome levels (**a**) or mRNA levels (**b**). **c** N2AFOXF1 cells were untreated or treated with DOX for 42 h, then infected (MOI = 2) for 5 h before ChIP-qPCR analysis of histone H3 or the indicated modifications at the viral genomic loci indicated at the bottom. The occupancies of the modifications were normalized to those of H3. **d** Neuro-2a cells were transfected with 600 ng/mL of the indicated plasmids for 42 h, then infected (MOI = 2) for 6 h before ChIP-qPCR analysis of histone H3 and H3K27ac at the indicated viral genomic loci. **e** Neuro-2a cells were transfected with 200 ng/mL pFOXF1 or pcDNA for 42 h, then infected (MOI = 1) for 3 h before ATAC-seq analysis. Percentages of viral reads in total reads are shown. **f** Based on the ATAC-seq data, a volcano plot depicts differential chromatin accessibility in viral (red) and host (black) promoter regions. Each point represents a promoter. **g** Neuro-2a cells transfected with 50 ng/mL plasmids, then infected (MOI = 5) for 5 h. Upper, representative immunofluorescence images show ATRX (green), Flag (red) and DAPI-stained nuclei (blue). Lower, fractions of cells with puncta in Flag-positive or Flag-negative cells in pFOXF1-Flag (left) or pFOXK1-Flag (right) transfected cells. One point represents one visual field. ICP0-null HSV-1 was used throughout the figure. n = 2 (**e**, **f**), 3 (**a**, **c**, **d**) or 4 (**b**) biologically independent samples. Data were analyzed by two-way ANOVA with Sidak's multiple comparisons tests (**a**–**d**) or two-tailed unpaired t tests (**g**) and are presented as mean ± SD. Source data are provided as a Source Data file.

H3K27ac/H3 on the *ICP27* and *UL22* sites (Supplementary Fig. 6a, other panels). At 5 hpi, FOXF1 decreased total H3 on all sites (Fig. 5c, left panel) and H3K9me3/H3 on most sites but increased H3K18ac/H3 and H3K27ac/H3 on all sites (Fig. 5c, other panels). We also analyzed host FOXF1 target sites in *Fos* and *Etv1* genes identified in our ChIP-seq data. Although FOXF1 did not reduce H3 or H3K9me3/H3 on these sites, it did increase H3K18ac/H3 and H3K27ac/H3 on the *Etv1* site, and possibly on the *Fos* site (a trend without significance) (Supplementary Fig. 6b) suggesting that inducing histone acetylation may be a FOXF1 function applicable to both viral and host genes. We then tested the effects on the viral chromatin further by transfection in Neuro-2a cells and observed decreases in total H3 but increases in H3K27ac/H3 on all

the viral sites tested induced by transfected FOXF1 relative to both the empty vector and an irrelevant FOX protein, FOXP1 (Fig. 5d).

The above results strongly indicate that, starting very early during infection, FOXF1 could induce the removal of H3 and H3K9me3 from HSV-1 chromatin while promoting acetylation of the remaining H3. Since all these effects are consistent with chromatin opening, we then performed assays for transposase-accessible chromatin with sequencing (ATAC-seq). At 3 h after ICP0-null virus infection of Neuro-2a cells, transfected FOXF1 increased viral reads relative to total reads associated with accessible chromatin (Fig. 5e), and increased accessibility in all viral promoter regions (Fig. 5f). However, signals were increased globally (Supplementary Fig. 6c) along the viral genome without specific peaks like those in the ChIP-seq data suggesting that even though DNA association is partially sequence-specific, the effects on accessibility are non-specific and global.

Such effects made us wonder whether PML-NBs that colocalize with the HSV-1 genome might be affected[48,49]. Indeed, while basically all control cells showed clear ATRX puncta representing PML-NBs, overexpressed FOXF1 but not FOXK1 caused almost total dispersal of the puncta in ICP0-null virus infected Neuro-2a cells (Fig. 5g). Although these results may be an artifact of FOXF1 overexpression, we note that because PML-NBs contain multiple repressive chromatin remodelers, such as ATRX and DAXX[16,50], dispersal of PML-NBs is also in line with activation of viral chromatin.

Activating FOX proteins generally associate with CBP/P300

To understand how FOX proteins modulate viral chromatin, we first considered the observation that FOXA1 binds core histones[33]. Therefore, we pulled down transfected FOXA1, C1, E1, F1 and K1 after Benzonase treatment to digest DNA (Supplementary Fig. 7a) and observed co-immunoprecipitation of histone H3 with all of them (Supplementary Fig. 7b). An H3 antibody also immunoprecipitated transfected FOXF1 (Supplementary Fig. 7c). The association with FOXF1 depended on aa200–380 but not the DBD (Supplementary Fig. 7d) consistent with the observation that FOXA1 uses a non-DBD domain to interact with H3[33]. However, since both activating and repressive FOX proteins associate with H3, this association cannot explain the activating or repressive activities.

To explore binding partners involved in the regulatory activities, we conducted proximity-labeling[51] using FOX proteins fused to TurboID to label proximal proteins by biotin (Fig. 6a, Supplementary Fig. 8a), which were pulled down using streptavidin beads and analyzed by liquid chromatography with tandem mass spectrometry (LC-MS/MS). FOXF1-TurboID were compared with three negative controls, FOXK1-TurboID, FOXF1Δ200–380-TurboID, and unfused TurboID. Immunofluorescence assays demonstrated nuclear localization of all TurboID-FOX fusion proteins (Supplementary Fig. 8b). After transfection and infection of Neuro-2a cells, comparisons with the three controls commonly identified 53 potential interactors (Fig. 6b, Supplementary Fig. 8c). Kyoto Encyclopedia of Genes and Genomes (KEGG) database analysis shows that these proteins are predominantly related to ATP-dependent chromatin remodeling (Supplementary Fig. 8d). Application of a more stringent threshold resulted in 11 proteins (Fig. 6b), which form an interaction network according to the STRING database (Supplementary Fig. 8e). Interestingly, homologous histone acetyltransferases CBP and P300[52], known to stimulate gene transcription by histone acetylation, were both among these 11 proteins. Therefore, we tested their association with FOX proteins further. After Benzonase treatment, co-transfected FOXF1-HA and CBP-Flag were both co-immunoprecipitated by HA and Flag antibodies (Fig. 6c). Immunoprecipitation of transfected FOXF1 pulled down endogenous CBP, too (Fig. 6d). Transfected CBP also co-immunoprecipitated with transfected FOXA1, C1 and E1, but not with FOXK1 or FOXF1Δ200–300 (Fig. 6e, Supplementary Fig. 9). Therefore, activating but not repressive FOX proteins generally associate with CBP/P300.

FOXF1 recruits CBP/P300 to acetylate histones in HSV-1 chromatin and stimulate viral gene transcription

Next, we examined the effects of these FOXF1 proximal proteins. We knocked down each of these except TTN, which is not implicated in gene regulation (NCBI database), and found that siRNAs that effectively knocked down BCL9L, CREBBP (CBP), EP300 (P300) or ARID1A (Supplementary Table 1) decreased viral yields in FOXF1 overexpressing cells, and a second set of siRNAs confirmed the effects of CBP, P300 and ARID1A but not BCL9L (Fig. 6f). We then focused on CBP/P300. Surprisingly, in the absence of FOXF1, both dual knockdown of CBP and P300 and a specific CBP/P300 inhibitor (A-485)[53] substantially increased yields of both ICP0-null and WT HSV-1 at 48 hpi indicating that CBP/P300 normally suppresses HSV-1 replication perhaps indirectly (Fig. 6g, h, Supplementary Fig. 10a, b), such that the differences between viral yields in the presence and absence of FOXF1 were eliminated or greatly reduced. This suggests that FOXF1 requires CBP/P300 to efficiently activate HSV-1 replication. Even at 3 hpi, the dual knockdown greatly attenuated the stimulation of viral gene expression by FOXF1 (Supplementary Fig. 10c) suggesting that CBP/P300 acts at the early stage of transcription.

To test whether CBP/P300 mediates stimulation of viral chromatin acetylation by FOXF1 (Fig. 5c), we used A-485 in ChIP-qPCR assays. At 5 hpi, in the absence of FOXF1, A-485 had little effect on the baseline H3K27ac/H3 levels on the viral sites (Fig. 6i) and even increased H3K18ac/H3 on some sites (Supplementary Fig. 10d) suggesting that CBP/P300 does not acetylate HSV-1 chromatin without FOXF1. Remarkably, in the presence of FOXF1, A-485 significantly reduced H3K27ac/H3 on all viral sites tested, with stronger impacts on motif$^+$ than motif$^-$ sites. A-485 also decreased H3K18ac/H3 on the motif$^+$ but not motif$^-$ sites. Regardless, the increases in histone acetylation on viral sites caused by FOXF1 were largely eliminated by A-485 for both modifications, which strongly suggests that FOXF1 recruits CBP/P300 to acetylate histones associated with the HSV-1 genome.

FOXK1 associates with SIN3A and MAX to repress HSV-1 replication and antagonizes activating FOX proteins

To understand the repressive mechanisms of FOXK1, we re-used the proteomic data to identify proteins proximal to FOXK1-TurboID relative to FOXF1-TurboID and unfused TurboID, resulting in 85 proteins (Fig. 7a), among which MAX, KIN, GTF2A1, SIN3A and ARID4B are implicated in gene regulation (NCBI database). Among siRNAs for these genes, each of two siRNAs against MAX and one of two siRNAs against SIN3A increased ICP0-null HSV-1 yields in Neuro-2a cells overexpressing FOXK1 (Supplementary Table 1, Fig. 7b, Supplementary Fig. 11a). In FOXK1 KO cells, both SIN3A siRNAs eliminated virus suppression by transfected FOXK1 and both MAX siRNAs attenuated the suppression (Fig. 7c) suggesting that FOXK1 work with MAX and SIN3A to suppress HSV-1 replication. Because SIN3A is a scaffolding protein known to recruit histone deacetylases to chromatin[54], we further investigated the role of histone deacetylation. Interestingly, treatment with a histone deacetylase inhibitor trichostatin A (TSA), a chemical that can induce reactivation in neuronal culture models[55], not only increased viral yields substantially, but also weakened the suppressive effects of FOXK1 (Fig. 7d) suggesting that histone deacetylation is involved in FOXK1 function. Since the effects of MAX siRNAs were remarkably substantial, we also tried single guide RNAs (sgRNAs). All three sgRNAs effectively reduced MAX expression (Supplementary Fig. 11b) and caused ~2-log increases in viral yields (Fig. 7e), which further indicates that MAX strongly suppresses HSV-1 replication. Although we failed to co-immunoprecipitate FOXK1 with MAX or SIN3A (Supplementary Fig. 9), Western blotting of biotin-captured FOXK1 proximal proteins labeled using FOXK1-TurboID readily detected MAX and SIN3A (Fig. 7f) confirming their proximity to FOXK1. We note that previous studies reported FOXK1-SIN3A interactions in yeast two-hybrid and co-immunoprecipitation assays[56,57]. It is possible

https://doi.org/10.1038/s41467-026-68915-1

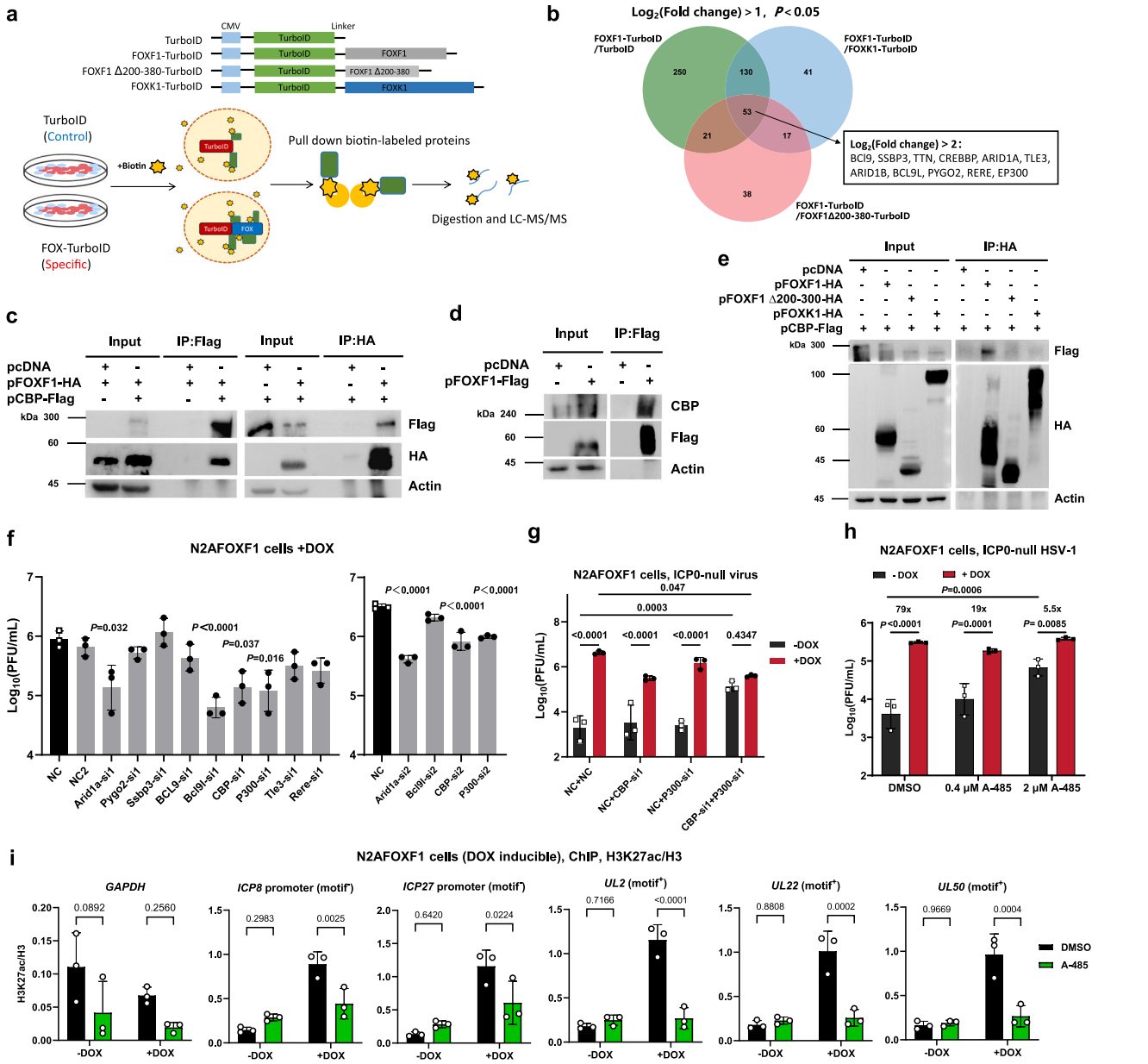


Fig. 6 | FOXF1 interacts with CBP/P300 to acetylate viral chromatin and activate viral replication. a Diagram of the proximity labeling experimental design. Neuro-2a cells were transfected with the indicated plasmids for 42 h, then infected with ICP0-null HSV-1 (MOI = 5) for 6 h before proximity labeling and mass spectrometry analysis. **b** Venn diagram of potential proximal proteins. Each circle represents the number of proteins identified by comparing the experimental group (pFOXF1-TurboID) with one negative control. **c**–**e** 293T cells were transfected (400 ng/mL) or co-transfected (400 + 400 ng/mL) with the plasmids indicated to the left for 36 h, then infected with ICP0-null HSV-1 for 5 h (MOI = 5). Cells were immunoprecipitated using the antibody indicated at the top, then analyzed by Western blots using the antibodies labeled to the right. The experiments were repeated twice with similar results. **f** N2AFOXF1 cells were treated with DOX and transfected with 60 nM siRNA for 48 h, then infected with ICP0-null HSV-1 (MOI = 0.2) for 48 h before virus titration. NC, negative control. The *P* values indicate differences compared to NC. **g** N2AFOXF1 cells were treated with DOX and co-transfected with various siRNA combinations (40 + 40 nM) for 48 h, then infected with ICP0-null HSV-1 (MOI = 0.2) for 36 h before virus titration. **h** N2AFOXF1 cells were untreated or treated with DOX and A-485 (or DMSO) for 24 h, then infected with ICP0-null HSV-1 (MOI = 0.2) for 32 h before virus titration. **i** N2AFOXF1 cells were untreated or treated with DOX and/or 2 μM A-485 (or DMSO) for 24 h, then infected with ICP0-null HSV-1 (MOI = 2) for 5 h before ChIP-qPCR analysis of H3K27ac occupancies normalized to H3 occupancies at the genomic loci indicated at the top. $n = 3$ (**a**, **b**, **f**–**i**) biologically independent samples. Data were analyzed by two-tailed unpaired t tests (**b**), one-way ANOVA with Dunnett's multiple comparisons tests (**f**) or two-way ANOVA with Sidak's multiple comparisons tests (**g**–**i**) and are presented as mean ± SD. Source data are provided as a Source Data file.

that these protein-protein interactions are transient, weak and/or indirect, so that they did not persist during our co-immunoprecipitation assay.

Given that FOXF1 associates with co-activators while FOXK1 is at least proximal to co-repressors and may function with them to repress HSV-1 replication, we wondered whether activating and repressive FOX proteins are antagonistic. Indeed, during co-transfection, FOXK1 abolished the strong effects of simultaneously expressed FOXA1 and E1, and greatly reduced the effects of FOXC1 and F1 on ICP0-null HSV-1 replication (Fig. 7g). Antagonism of FOXA1 was also achieved by FOXK2, but not by FOXP1, FOXH1, or the DBDs of FOXC1 or A1 (Fig. 7h) suggesting that non-DBD domains are required for the antagonism. Therefore, FOXK proteins work with repressive cofactors to antagonize activating FOX proteins.

https://doi.org/10.1038/s41467-026-68915-1

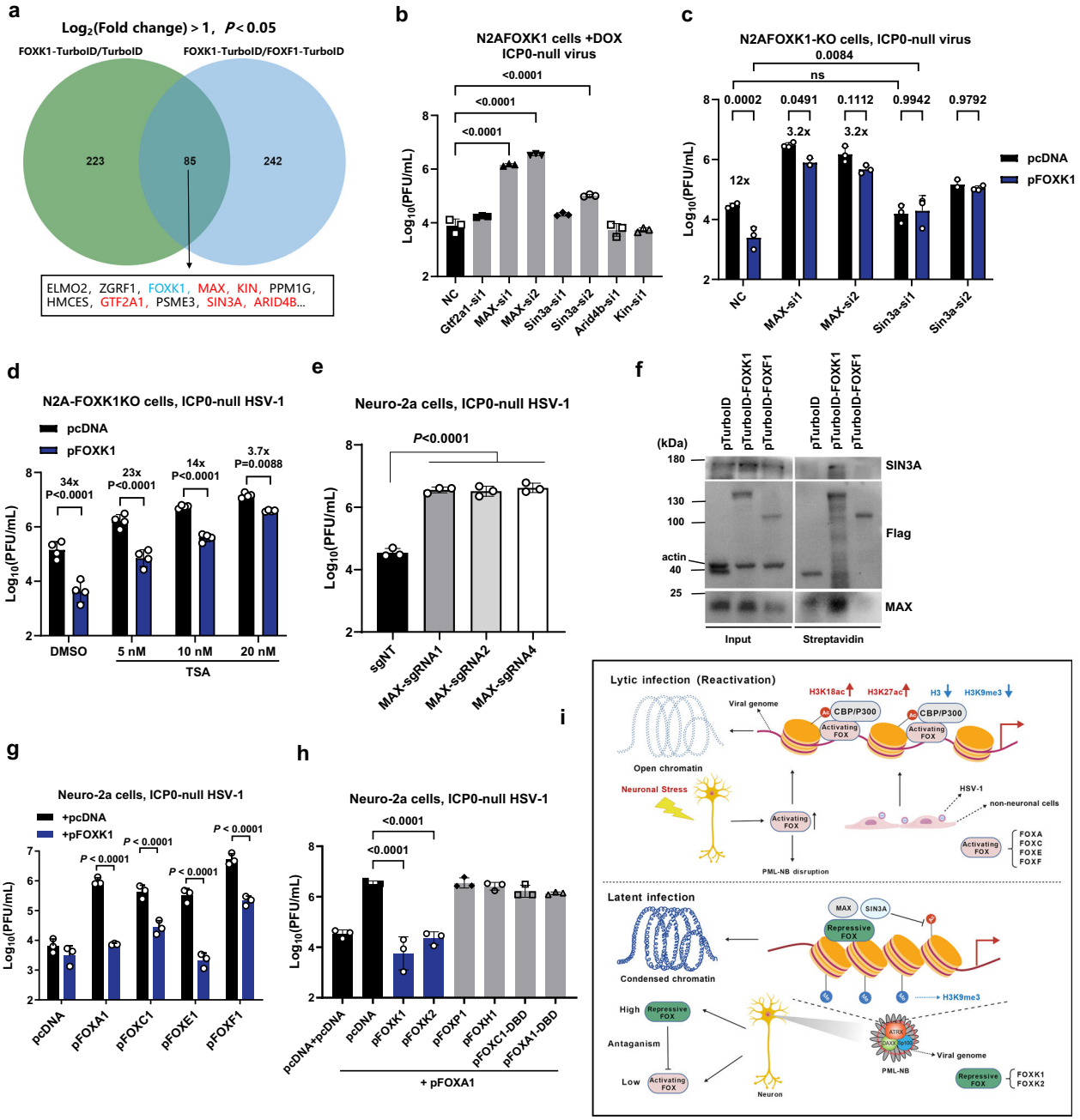


Fig. 7 | FOXK1 works with repressive factors and antagonizes activating FOX proteins. a Venn diagram of proteins identified by comparing the pFOXK1-TurboID group with the control groups in the proximity labeling data. In red are selected genes for functional studies. **b** N2AFOXK1 cells were treated with DOX and transfected with 60 nM siRNA for 48 h before infection. **c** N2A-FOXK1KO cells were transfected with 60 nM siRNAs for 24 h, then transfected with 200 ng/mL plasmid for an additional 24 h before infection. **d** N2A-FOXK1KO cells were transfected with 200 ng/mL plasmid, then treated with DMSO or the indicated concentrations of TSA for 20 h before infection. **e** Neuro-2a cells were transfected with 400 ng/mL plasmids expressing various sgRNAs targeting MAX for 24 h before treatment with 2 μg/mL puromycin. Four days later, cells were infected. The *P* value indicates the difference between each sgRNA and the control. **f** 293T cells were transfected with 400 ng/mL plasmids for 42 h, infected for 6 h (MOI = 5), then labeled with biotin. Biotinylated proteins were pulled down by streptavidin beads and analyzed by Western blots. The experiment was repeated once with similar results. **g**, **h** Neuro-2a cells were co-transfected with the plasmid combinations (150 + 150 ng/mL), then infected. **i** A diagram summarizing the model proposed by this study, created with biogdp.com. All infections used ICP0-null HSV-1 (MOI = 0.2) and lasted for 48 h before virus titration unless otherwise specified. $n = 3$ (**a**–**c**, **e**, **g**, **h**) or 4 (**d**) biologically independent samples. Data were analyzed by two-tailed unpaired *t* tests (**a**) one-way ANOVA with Dunnett's multiple comparisons tests (**c**, **e**, **h**) or two-way ANOVA with Sidak's multiple comparisons tests (**d**, **g**) and are presented as mean ± SD. Source data are provided as a Source Data file.

Discussion

These studies identified two sets of host proteins within one family with opposing effects on the viral lytic-latent balance. Interestingly, their expression profiles correlate with the viral phenotypes of latency or replication in that neurons express repressive *Fox* genes highly but activating *Fox* genes poorly consistent with favorable conditions for latency, while non-neuronal cells or stressed neuronal cells display high or increased expression of certain activating *Fox* genes correlating with lytic infection in such cells. Strikingly, both knockdown/knockout of FOXK1 and overexpression of activating FOX proteins are sufficient to

induce reactivation indicating that HSV-1 latency requires optimal FOX protein composition provided by neurons. Moreover, certain activating *Fox* genes are quickly and substantially upregulated by certain reactivation-related stresses suggesting that stress-induced activating FOX proteins might be involved in the initial steps of reactivation. Thus, these results introduce the notion that the viral lytic-latent balance is controlled by counteracting host factors, whose optimal composition provided by specific host cells is required for latency and perturbation of the composition by stresses can induce reactivation.

What are the mechanisms by which these FOX proteins regulate the lytic-latent balance? Our data converge into a model wherein these proteins extensively bind the viral genome at least partly through nonsequence-specific interactions and regulate viral chromatin and gene transcription through cofactors (Fig. 7i). The importance of non-specific DNA interactions is not unprecedented since such binding of FOXA proteins to the cellular chromosome has been reported to contribute to gene reactivation post-mitosis[58,59]. Some other pioneer factors have also been observed to bind nucleosomes via non-specific DNA interactions or partial DNA motifs[60]. Moreover, like FOXA1[33,61], we show that other FOX proteins can also associate with H3 independent of DNA, which should strengthen the presumably weak non-specific DNA interactions. Notably, interactions with core histones have been shown to contribute to chromatin opening by FOXA proteins[61]. Although most of the other activating FOX proteins are not formally known as pioneer factors, their ability to reactivate the latent virus, a process involving opening of condensed viral chromatin[62], as well as their extensive use of non-specific DNA interactions, is consistent with pioneer transcription factor activities[63].

Although they commonly associate with viral DNA, activating and repressive FOX proteins function with distinct cofactors to regulate HSV-1 replication. Activating FOX proteins generally interact with histone acetyltransferases CBP and P300, and at least FOXF1 enhances viral gene expression and histone acetylation through these enzymes. Acetylation reduces the affinity of histones for DNA by neutralizing the positive charge of lysine, thereby increasing chromatin accessibility[64]. Accordingly, FOXF1 can globally enhance HSV-1 chromatin accessibility. We note that the FOXF1 proximal proteins appear to form an interaction network (Supplementary Fig. 8e), within which ARID1A, besides CBP and P300, is required for efficient HSV-1 activation (Fig. 6f) raising the possibility that FOXF1 recruits a complex for gene activation. On the other hand, FOXK1 is proximal to a different set of proteins, among which at least SIN3A and MAX work with FOXK1 to repress HSV-1 replication. It is intriguing that activating and repressive FOX proteins associate with histone acetyltransferases (CBP/P300) and a cofactor of deacetylases (SIN3A) respectively and antagonize each other. MAX is primarily known as a MYC cofactor[65], but we did not detect MYC in our proteomics data. The mechanism by which MAX suppresses HSV-1 replication so strongly is unknown but highly worthy of investigation in future.

Latency is a feature shared by many DNA viruses and retroviruses. Given the non-specific DNA interactions, the activating or repressive FOX proteins might also regulate the lytic-latent balance of other viruses. Indeed, neuronal replication of multiple alphaherpesviruses could be significantly affected by FOXF1 and FOXK1 (Supplementary Fig. 2). However, FOXK1 and K2 were reported to promote KSHV replication[35,36] in contrast with their repressive role in HSV-1 neuronal replication suggesting that FOX proteins regulate viral infection and/or latency in a context-dependent manner. More work is needed to further elucidate the role of FOX proteins in the viral lytic-latent balance.

Methods

Cells

Vero (catalogue no. CCL-81), 293T (catalogue no. CRL-3216), U2OS (catalogue no. HTB-96), HFF (catalogue no. CRL-1634), and Neuro-2a (catalogue no. CCL-131) cells were obtained from American Type Culture Collection and maintained in Dulbecco's modified Eagle's medium (DMEM) supplemented with 5% newborn calf serum (for Vero cells) or fetal bovine serum (for other cells) at 37°C in 5% CO_2. Mouse TG neurons were isolated and cultured according to a reported protocol with slight modifications[66]. Briefly, 6-week-old male Institute for Cancer Research (ICR) mice (Shanghai Laboratory Animal Center) were anesthetized with isoflurane (RWD Life Science) for 1 min and transcardially perfused with 10 ml of phosphate buffered saline (PBS). TG were dissected and digested for 1 h at 37 °C in a collagenase/dispase II solution (Sigma-Aldrich, C9891 and D4693). Neurons were isolated in an OptiPrep gradient (Sigma-Aldrich, D1556), counted and seeded onto 10-mm coverslips coated with poly-D-lysine (Sangon Biotech, catalog number: E607014-0002) and laminin (Sigma-Aldrich, catalog number: L2020) in Neurobasal-A medium (Thermo Fisher Scientific, catalog number: 10888022). Approximately 5000 neurons were plated on each coverslip. One hour after seeding, the coverslips with neurons were transferred to a 48-well plate and cultured in Neurobasal-A medium supplemented with 2% N21 (Bio-Techne, AR008), 50 ng/mL β-neuronal growth factor (Novoprotein, C060), 50 ng/mL glial-derived neurotrophic factor (Novoprotein, C060), C226) and 1 mg/mL mitomycin C (MedChemExpress, hay-13316) for two to three days before use. Neurogenin3 inducible human iPSCs (iNGN3 iPSCs)[67] kindly provided by George Church of Harvard Medical School were differentiated into neurons for the experiment in Fig. 2a as described previously[21,23], or for the experiment in Supplementary Fig. 3a using another previously described method[42] as follows: Briefly, iNGN3 iPSCs were seeded in Matrigel (STEMCELL)-coated 6-well plates (Corning or Costar, 1×10^6 cells) and NGN3 was induced using doxycycline (Dox, 1 μg/mL)-containing mTeSR media with supplement (STEMCELL) for 3 days. The medium was replaced with mTeSR/N2 media (mTeSR+supplement:Neurobasal plus+N2 supplement (Thermo Fisher Scientific) =1:1) containing five inhibitors (5i; LDN193189 (APExBIO, 0.1 μM), SB431542 (APExBIO, 10 μM), DAPT (APExBIO, 10 μM), SU5402 (APExBIO, 10 μM), and CHIR99021 (APExBIO, 5 μM) for 5 days with daily replacement. After 5i treatment, the cells were re-plated to poly-L-ornithine (50-100 μg/mL, Sigma)/laminin (10 μg/mL, Gibco) coated plates and further differentiated in 4 G media [4 G: BDNF, GDNF, β-NGF, and NT-3 (all 10 ng/mL, PeproTech), ascorbic acid (0.2 mM) in Neurobasal plus (supplemented with B27 plus, Thermo Fisher Scientific):DMEM/F12 (Thermo Fisher Scientific)=(1:1)]. The cells were incubated with 5-fluoro-2'-deoxyuridine (20 μM, FUdR, RPI) for 7 days to eliminate undifferentiated dividing cells and maintained in 4 G media thereafter.

Viruses

HSV-1 strain KOS, HSV-2 strain 186 and ICP0-null mutant (7134) HSV-1 derived from KOS[41] were propagated and assayed as described previously[23]. Basically, wild-type HSV-1 and HSV-2 were propagated and titrated in Vero cells, and ICP0-null HSV-1 was propagated and titrated in U2OS cells. PRV and BoHV-1 were generous gifts from Zhengfei Liu at Huazhong Agricultural University[68]. BoHV-1 was originally from Shafiqul Chowdhury of Louisiana State University[69]. PRV was propagated and titrated in PK15 cells, which were kindly provided by Yaowei Huang of Zhejiang University. BoHV-1 was propagated and titrated in MDBK cells kindly provided by Liqian Zhu at Hebei University. VZV bacterial artificial chromosome (BAC) DNA was a kind gift from Hua Zhu of Rutgers University[70] and purified as described previously[20]. Recombinant HSV1FOXC1, HSV1FOXC1delAD and HSV1FOXC1delADb viruses were constructed in our laboratory, as described previously[21]. For infection of cell culture, the viruses were added to cells at the indicated MOIs, incubated for 1 h at 37 °C with gentle shaking every 15 min for adsorption. Then the cells were washed once with PBS and the supernatants were replaced with fresh media before further incubation at 37 °C. Viral titers were determined by

regular plaque assays. For $TCID_{50}$ assays of BoHV-1, Neuro-2a cells were seeded in 96-well plates and infected when the cells reached 60% confluency. BoHV-1 was diluted in a 10-fold serial dilution using serum-free DMEM medium, with eight replicates per dilution gradient. The diluted BoHV-1 was added to Neuro-2a cells. After 1 hour of infection, the culture medium was supplemented with a final concentration of 2.5% fetal bovine serum. Cytopathic effects were observed daily. At 7 dpi, cells were fixed and stained with crystal violet, wherein non-viable cells remained unstained. $TCID_{50}$ values were calculated using the Reed–Muench method. All viral infection procedures were performed in a biosafety level 2 laboratory.

Plasmids

All *Fox* genes were cloned into the Flag-HA-pcDNA3.1- (here referred to as pcDNA) vector. The coding sequences were amplified from cDNA derived from 293T or Neuro-2a cells by PCR as previously described[21]. We also removed the Flag tag in the pcDNA vector to generate the pcDNA-HA vector, into which we cloned the genes encoding FOXF1, FOXK1, FOXF1Δ200–300, FOXA1, FOXC1, and FOXE1 for co-immunoprecipitation assays. All mutations were introduced into the plasmids using a Q5 Site-Directed Mutagenesis Kit (NEB #E0554). The coding sequences of *Foxk1* and *Foxf1* were cloned into pTRIPZ, a Dox-inducible lentiviral expression vector (Addgene #206981) to construct pTRIPZ-FOXF1 and pTRIPZ-FOXK1 plasmids. To construct the FOXK1 and FOXK2 shRNA plasmids, we selected the target sequences 5′-GGAGCCTCACTTCTATCTTCG-3′ and 5′-CCA-GAGCTCAAGCGAGTTAAA-3′. The sequences were annealed and inserted into the pLKO.1 vector (Addgene #128073). To construct different lentiviral plasmids, the coding regions of *Foxa1*, *Foxc1*, *Foxe1*, *Foxf1* and *Foxk1* genes were cloned into pLVX-EF1α-IRES-mCherry (Addgene) vector using BamHI and XbaI restriction sites. To construct MAX-knockout sgRNA plasmids, we designed the target sequence using the Synthego online tool (https://design.synthego.com/#/) (Supplementary Table 2). The complementary oligonucleotides were annealed and subsequently cloned into the LentiCRISPRv2 vector (Addgene #98290) via the BsmBI restriction site. Primer sequences used for cloning are listed in the Supplementary Table 2.

Transfection

Plasmids, VZV BAC DNA or siRNAs were transfected into cells using a Lipomaster 3000 transfection reagent (Vazyme Biotech Co., TL301-01) according to the manufacturer's instructions. For small scale transfection, cells were seeded in 24-well plates at a density of 1.5×10^5 cells per well and transfected six hours later with 100–200 ng of plasmids or 30 pmol of siRNA per well, as specified in figure legends. For co-transfection of VZV BAC DNA and plasmids, 100 ng of VZV BAC DNA and 150 ng of a plasmid were added to each well of a 24-well plate. For immunoprecipitation, ~10^7 cells in a 100-mm plate were transfected with 4 μg of plasmid per plate, or 4 μg + 4 μg of plasmid for co-transfection. siRNAs were synthesized and purchased from Qingke Biological Company, and their sequences, as well as knockdown efficiencies calculated from target mRNA levels quantified by RT-qPCR, are provided in Supplementary Table 1.

Western blot analysis

Cells were lysed in an SDS-PAGE sample loading buffer: 10 mM Tris-HCl (pH 8.0), 50 mM dithiothreitol (DTT), 1% SDS, 10% Glycerol, 0.008% bromophenol blue. Proteins were resolved on 10–12% SDS-polyacrylamide gels and transferred to polyvinylidene fluoride membranes (Millipore #IPVH00010) before being probed with the following antibodies at the following dilutions. Primary antibodies: anti-Flag M2 antibody (1:2000, sigma #F1804); anti-HA antibody (1:2000, Sangon Biotech #D110004-0100); anti-actin antibody (1:10000, ABclonal #AC026); anti-H3 antibody (1:2000, Solarbio #K200033M); anti-FOXK1 antibody (1:1000, invitrogen PA5-36257); anti-FOXK2 antibody (1:1000, ABclonal #A14245); anti-CREBBP antibody (1:1000, Cell Signaling Technology #7389 s); anti-H3K27ac antibody (1:2000, Abcam #ab4729); anti-ARID1A antibody (1:2000, Proteintech #83733-3-RR); anti-PML antibody (1:500, Merck #05-718); anti-MAX antibody (1:2000,Proteintech, #10426-1-AP, for Fig. 7f); anti-MAX antibody (1:2000, Abcam #ab199489, for other experiments); anti-SIN3A antibody (1:1000, Proteintech #67197-1-Ig); anti-FOXC1 antibody (1:1000,Abcam #ab227977); anti-FOXA1 antibody (1:1000, Proteintech #20411-1-AP); anti-FOXF1 antibody (1:1000,Abcam #ab168383); anti-ICP0 antibody (1:1000, Santa Cruz #sc-53070). Secondary antibodies: HRP-conjugated goat anti-mouse (1:4000, SouthernBiotech #1030-05) and goat anti-rabbit antibodies (1:4000, SouthernBiotech #4030-05).

Lentivirus production

Four μg of lentiviral transfer plasmid, 3.8 μg of psPAX2 plasmid (Addgene), and 1.9 μg of pMD2.G plasmid (Addgene) were transfected into 293T cells in a 100 mm dish using ExFect transfection reagent (Vazyme Biotech Co., T101-02). At 16 h post-transfection, the culture medium was replaced with fresh medium. At 48 h post-transfection, the supernatant containing lentivirus was collected and stored at 4 °C, after which fresh medium was replenished. At ~92 h post-transfection, a second batch of supernatant was collected and combined with the first batch. The pooled supernatant was centrifuged at 400 × *g* for 5 min to remove cell debris and filtered through a 0.45 μm syringe filter (Jet Bio-Filtration #FPV-403-030) to further clarify the solution. Lentiviral particles were concentrated by ultracentrifugation using a 50 Ti rotor (Beckman Coulter) at 110,000 x *g* for 90 min. The concentrated lentiviral particles were re-suspended in the medium suitable for the next step and stored at -80 °C for long-term preservation.

Construction of N2AFOXF1, N2AFOXK1 and N2A-FOXK1KO cells

Lentivirus expressing FOXK1 or FOXF1 derived from pTRIPZ-FOXF1 or pTRIPZ-FOXK1 plasmid was transduced into Neuro-2a cells in the presence of 8 μg/ml polybrene (Sigma). Twenty-four h later, the supernatant was replaced with fresh medium containing 2 μg/ml puromycin. Puromycin-resistant cells were selected over a period of 10–14 days, during which time the medium was changed every 48 h. Stable expression of FOXK1 and FOXF1 was confirmed by Western blotting. To induce the expression of FOXK1 or FOXF1, cells were treated with 1 μg/ml doxycycline hydrochloride (Solarbio #D8960) for at least 24 h. N2A-FOXK1KO cells were constructed by CRISPR-Cas9 technology as described previously[71]. Briefly, sgRNA was designed based on the mouse *Foxk1* gene sequence with the aid of the online resource https://zlab.bio/guide-design-resources. The selected target sequence was 5′-GCCGAAGUCGGCGAGGACAG-3′. The sgRNA sequence was cloned into the PX459 vector (Addgene). Neuro-2a cells were seeded in a 24-well plate and transfected with the sgRNA expressing plasmid. At 24 h post-transfection, the supernatant was replaced with fresh medium, and cells were transfected again with the same plasmid. Twenty-four h later, the supernatant was replaced with fresh medium containing 2 μg/ml puromycin. At 48 h after adding puromycin, cells were trypsinized and seeded in 96-well plates with a density of 0.5 cells per well in the presence of 1 μg/ml puromycin to expand single colonies. When cells grew to confluency, they were trypsinized and transferred to large wells or plates for further propagation in the presence of 1 μg/ml puromycin. Successful knockout of FOXK1 was confirmed by Western blotting.

RNA-seq analysis of iPSC-derived neurons

Twenty-one days after seeding at 1×10^5 cells/well on Poly-L-ornithine/laminin coated plates, iNGN3 iPSC-derived neurons were mock-infected or infected with HSV-1 strain KOS at MOIs of 10 or 1 at 37 °C for 2 h. The inocula were removed, the cells were washed with DMEM/F12, and fresh prewarmed 4 G medium was added. At 10 hpi, for each sample, RNA was harvested from four wells of cultured neurons

using an RNeasy Plus Mini Kit (Qiagen Catalog#74134). The culture medium was removed, and 100 µl of lysis buffer provided in the kit was added to each well. Genomic and viral DNA were eliminated by treatment with the gDNA Eliminator Spin Columns supplied in the kit followed by RNA extraction according to the manufacturer's protocol. Extracted RNA samples were quantified using a NanoDrop ND-1000 Spectrophotometer (ThermoFisher Scientific, USA), and RNA integrity was assessed using an Agilent 2100 Bioanalyzer (Agilent Technologies, CA, USA). RNA sequencing libraries were prepared using the NEBNext Ultra II RNA Library Prep Kit for Illumina (New England Biolabs Catalog#E7760S) following the manufacturer's instructions. Oligo(dT) enrichment was performed as the first step of library preparation using the NEBNext Poly (A) mRNA Magnetic Isolation Module (New England Biolabs Catalog#E7490S), followed by fragmentation and first and second-strand cDNA synthesis. After adapter ligation and index addition followed by PCR, libraries were analyzed for length and concentration using the Agilent Bioanalyzer and qPCR, and 200 bp Paired-End sequencing was performed using a NextSeq High-Output−Illumina HiSeq instrument by the BPF NGS Genomics Core Facility, Harvard Medical School. The human hg38 reference genome was first used for aligning fastq reads using STAR (version 2.7.11a)[72]. Transcript abundances were then quantified using Salmon[73] (version 1.10.2), and scaled by library size using tximport in the R package[74] (version 1.26.1), with each gene then normalized to transcripts per million (TPM) counts. The expression values of selected *Fox* genes were then selected and visualized using ComplexHeatmap in the R package[75] (version 2.14.0). Raw data have been uploaded to the NCBI GEO repository under access number GSE299792.

qPCR and RT-qPCR

To quantify HSV-1 genomes, total DNA was purified using a FastPure Cell/Tissue DNA Isolation Mini kit (Vazyme Biotech Co., #DC102-01) and a segment of the HSV-1 *TK* gene was assayed. Purified viral genomes of known concentrations as described previously[20] were serially diluted to generate standard curves for determination of genome copy numbers. Viral genome levels were normalized to mouse *Adipsin* gene levels. To quantify mRNAs, total RNA was purified using a FastPure Cell/Tissue total RNA isolation kit V2 (Vazyme Biotech Co., #RC112-01). For co-purification of DNA and RNA, a DNA/RNA co-extraction kit (TIANGEN, #A0722A) was used. RNA was reverse transcribed using a HiScript II Q RT SuperMix for qPCR (+gDNA wiper) kit and oligo(dT) primer according to the manufacturer's instructions (Vazyme Biotech Co, #R233-01). Serially diluted total RNA was used to generate standard curves for calculation of relative quantities. For quantifying *Fox* mRNAs in TG, absolute mRNA copy numbers were estimated by cDNA copy numbers, assuming that reverse transcription was efficient. For standard curves, regular PCR was first performed using the same pair of primers as for qPCR. The PCR product was purified using a HiPure Gel DNA Mini kit (Magen #D2111-03) and quantified by a spectrophotometer before being serially diluted and used as standards. *GAPDH* mRNA was used as an internal control for normalizing mRNA levels. For both DNA and RNA quantification, PCR reactions were prepared using a ChamQ Universal SYBR qPCR Master Mix (Vazyme Biotech Co., #Q711-02) and performed on a QuantStudio 3 real-time PCR system instrument (Applied Biosystems). qPCR primer sequences are listed in Supplementary Table 3.

Mouse procedures

All mouse housing and experimental procedures were in compliance with national ethical guidelines and approved by the Laboratory Animal Welfare and Ethics Committee of Zhejiang University with an approval code of ZJU20210251. Mouse infections were performed in an animal biosafety level 2 laboratory. Mice were housed at ambient temperature (~23 °C) with low humidity in an air-conditioned room with 12 h light-dark cycles. All experiments used male mice because female Avil$^{Cre+/-}$ mice were reported to exhibit *Cre* expression in oocytes according the information from the manufacturer (https://www.jax.org/strain/032536)[45]. ICR mice were obtained from the Shanghai Laboratory Animal Center. Genetically modified mice based on the C57BL/6 J strain were generated as described below. For HSV-1 infection, six-week mice were anesthetized with a solution containing 4 mg/ml sodium pentobarbital and 500 µg/ml xylazine hydrochloride, followed by inoculation of WT HSV-1 strain KOS on scarified corneas. The viral dose was 2×10^5 PFU/eye for ICR mice and 2×10^6 PFU/eye for the C57BL/6 J strain. For tear film viral titer determination, mice were anesthetized using 3% isoflurane (RWD Life Science) in oxygen at a flow rate of 0.5 ml/min with a V1 Table Top anesthesia machine (Colonial Medical Supply), and ocular swabs were collected using cotton-tipped applicators. For analysis of infectious viral titers in TG, mice were euthanized by cervical dislocation and TG were harvested and then homogenized in cell culture medium, subjected to three freeze/thaw cycles before titration by plaque assays. For quantification of DNA or RNA, TG was harvested in the same way and then homogenized in the lysis buffer for DNA or RNA purification before qPCR or RT-qPCR analysis as described above. For explant-induced reactivation, TG were excised and placed in a 12-well plate containing 1 ml of culture medium at 37 °C. Supernatants were collected and replenished daily. The collected supernatants were added to Vero cells to assess the presence of infectious virus by cytopathic effects.

Construction of sensory neuron-specific FOXK1 knockout mice

C57BL/6 JGpt-Foxk1^{em1Cflox} (Foxk1$^{f/f}$) mice with the Foxk1 gene flanked by loxP sites were obtained from GemPharmatech (Strain No. T014811). Avil$^{Cre+/-}$ mice (JAX Laboratory Strain No. 032536) that express Cre specifically in sensory neurons[45], also in the C57BL/6J background, were kindly provided by Liang Wang at Zhejiang University School of Medicine. The mice were housed and bred in the isolation barrier facility of the Laboratory Animal Center at Zhejiang University. Foxk1$^{f/f}$ mice were crossed with Avil$^{Cre+/-}$ mice to generate Avil$^{Cre+/-}$Foxk1$^{f/f}$ mice. For offspring genotyping, toe samples were collected, lysed in 200 µL of 50 mM NaOH at 99 °C, and then neutralized with 20 µL of 1 M Tris-HCl (pH 6.8). The lysates were centrifuged at 13,800 × *g* for 5 min, and the supernatants were used for PCR to identify genotypes. PCR primer sequences for genotyping are listed in Supplementary Table 4.

HSV-1 latency and reactivation in primary mouse TG neurons

To establish HSV-1 latent infection, two days after isolation and culture of TG neurons, neurons were treated with 100 µM ACV. On the next day, neurons were infected with a genetically engineered HSV-1 expressing GFP (64-GFP)[76] at an MOI of 20 in the presence of 100 µM ACV. The supernatant was replaced with fresh medium containing 100 µM ACV at 2 and 4 dpi. At 6 dpi, ACV was removed and replaced with regular medium for neuronal culture. At two days after ACV removal, neurons were transduced with lentiviruses at a dose of 1.5 x 10^8 genome copies per well in the presence of 2 µg/ml polybrene (Sigma-Aldrich). Lentiviruses were removed by medium replacement on the next day. Supernatants were collected every two days and assayed for infectious virus by evaluating cytopathic effects in Vero cells.

ChIP-seq

Neuro-2a cells were cultured in 100-mm dishes, transfected with 4 µg of pcDNA or pFOXF1 for 42 h, and then infected with ICP0-null HSV-1 for 5 h. Cells were crosslinked with 1% formaldehyde for 10 min and neutralized with 0.125 M glycine for 5 min, followed by two washes with 5 ml of ice-chilled PBS. Cells were collected into 15 ml conical tubes using 5 ml of cold PBS and centrifuged at 400 × *g* for 5 min at 4 °C. The resulting cell pellets were lysed in 300 µl of a lysis buffer (0.4% SDS, 10 mM of EDTA, 50 mM of Tris-HCl, pH 8.0) for 30 min before

being transferred to 1.5 ml Eppendorf tubes. The lysates were sonicated on ice using a SCIENTZ-IID ultrasonic homogenizer for six cycles of 1 min each, with a 30-sec on and 30-sec off interval, at a power output of 90 watts. A 10 μl aliquot of the sonicated lysate was used for analyzing DNA size distribution. This aliquot was incubated with 110 μl of water containing 0.2 M NaCl at 65 °C for 3–6 h to reverse crosslinking, followed by treatment with 0.2 mg/ml RNase A (Transgenic Biotechnology #GE101-01) for 1 h at 37 °C, then with 0.5 mg/ml proteinase K (Transgenic Biotechnology #GE201-01) for 1 h at 55 °C. DNA was purified using a HiPure Gel DNA Mini Kit (Magen #D2111-03). DNA size distribution was analyzed by agarose gel electrophoresis. This DNA sample also served as an input control. After an optimal DNA fragment size range of 100–500 bp was achieved, immunoprecipitation reaction was carried out by incubating 40 μl of FLAG affinity gel (Merck Millipore #F2426) and 280 μl of the sonicated cell lysate in 1 ml of ChIP dilution buffer [20 mM Tris-HCl (pH 8), 150 mM NaCl, 2 mM EDTA (pH 8), 1% Nonidet P-40, 0.1% sodium deoxycholate, and 0.01% SDS], supplemented with protease inhibitors (1 tablet per 50 ml, Roche #K562) with rotation for 3 h at 4 °C. The gel was washed sequentially with an ice-cold low-salt wash buffer, high-salt wash buffer, lithium chloride wash buffer, and TE buffer as described previously[23]. The cross-linked DNA-protein complexes were competitively eluted with a 3XFlag peptide (Beyotime #P9801). Crosslinking reversal and DNA purification were performed as described above. The purified input and immunoprecipitated DNA samples were submitted to Novogene for ChIP-seq high-throughput sequencing, followed by data analysis using protocols described previously[23]. Briefly, clean reads were aligned to the mm10+KOSnorepeat genome using Bowtie2 (version 2.3.4.3) with default parameters. Then the virus and mouse reads were split. DeepTools (version 3.5.1) bamCoverage was used to calculate read coverages. PlotProfiles and ComputeMatrix were utilized to plot signals around the TSS. The peak calling algorithm MACS2 (version 2.2.7.1) was used to identify significant peaks representing DNA binding sites for mouse and virus separately. The peaks were annotated to known genomic features using ChIPseeker (version 1.32.1). Homer2 (version 4.11.1) findMotifsGenome.pl was used to identify enriched known and de novo motifs. Integrative Genomics Viewer (version 2.16.2) was used to visualize read coverages. Raw data have been uploaded to the NCBI GEO repository under GEO access number GSE285910.

ChIP-qPCR

293T or Neuro-2a cells in 100-mm plates were infected or transfected then infected under conditions described in figure legends. The procedures for crosslinking, sonication and DNA purification were the same as described above for ChIP-seq. For analysis of DNA associated with FOXF1 and FOXK1 in Neuro-2a cells, the same procedure was also followed for immunoprecipitation. For analysis of DNA associated with histone H3 and its modifications, each immunoprecipitation reaction was conducted by incubation of 20-60 μl of the sonicated cell lysate, 20 μl of Dynabeads Protein A (Invitrogen #10002D) and 2 μg of antibody in 1 ml of ChIP dilution buffer with rotation overnight at 4 °C. For analysis of DNA associated with endogenous FOXF1 and FOXP1 in 293T cells, each immunoprecipitation reaction was carried out by incubating a mixture consisting of 100 μL of the sonicated cell lysate, 880 μL of ChIP dilution buffer, supplemented with protease inhibitor (1 tablet per 50 mL, Roche, cat. no. 4693132001), 20 μL of Dynabeads Protein A (Invitrogen, cat. no. 10001), and 3 μg of antiFOXF1 or anti-FOXP1 antibody or normal rabbit IgG, with rotation at 4 °C overnight. A-485 was from MCE (#HY-107455). The following antibodies were used: anti-histone H3 (Abcam #ab1791); anti-H3K27ac (Abcam #ab4729); anti-H3K18ac (Abcam #ab1191); anti-H3K9me3 (Abcam #ab8898); normal rabbit IgG (Merck Millipore #12-370); anti-FOXF1 (Abcam #ab168383); anti-FOXP1 (Abcam #ab134055). After washing, crosslinked DNA-protein complexes were eluted by incubation with 120 μl of elution buffer (1% SDS, 0.1 M $NaHCO_3$) at 65 °C for 10 min before crosslinking reversal and DNA purification as described above. Input and immunoprecipitated DNA samples were analyzed by qPCR using primers listed in Supplementary Table 3.

ATAC-seq

Neuro-2a cells were transfected with pFOXF1 for 42 h and infected with ICP0-null HSV-1 for 3 h at an MOI of 1. Cells were trypsinized, suspended in PBS and counted. A total of 5×10^4 cells were lysed by an ice-cold lysis buffer, consisting of 10 mM Tris-HCl (pH 7.4), 10 mM NaCl, 3 mM $MgCl_2$, and 0.1% (vol/vol) Igepal CA-630. DNA enzymatic reaction was performed using a TruePrep DNA Library Prep Kit V2 for Illumina (Vazyme Biotech Co., #TD501). VAHTS DNA Clean Beads (Vazyme Biotech Co., #N411-01) were used for purification of fragmented DNA, which was then used for library construction using a TruePrepTM Index Kit V2 for Illumina (Vazyme Biotech Co., TD202). The DNA library was submitted to Novogene for high-throughput sequencing. Data processing and analysis were conducted as previously described[23]. Raw data have been uploaded to the NCBI GEO repository under access number GSE285909.

Immunofluorescence assays

Cells were fixed in 4% paraformaldehyde for 10 min, washed with PBS for 5 min, permeabilized with 0.1% Triton X-100 for 10 min, and then washed three times with PBS for 5 min each. The cells were then incubated with 1% bovine serum albumin (BSA) in PBS for 1 h at room temperature. Primary antibodies were applied overnight in 1% BSA at 4 °C. After three washes with PBS for 10 min each, cells were incubated with secondary antibodies in 1% BSA for 1 h at room temperature. Nuclei were stained with DAPI solution (Solarbio #C0060) for 10 min, followed by three additional washes with PBS. Coverslips were sealed with an anti-fade mounting medium (Beyotime #P0126). The following antibodies and dilutions were used: anti-ATRX antibody (1:500, Abcam #ab97508); anti-PML antibody (1:500, Merck #05-718); anti-Flag M2 antibody (1:2000, Sigma #F1804); anti-Flag antibody (1:500, MBL #PM020); anti-ICP4 antibody (1:1000, Abcam #ab6514); anti-FOXC1 antibody (1:1000, Abcam #ab227977); goat anti-rabbit IgG Alexa Fluor 488 (1:500, Thermo Fisher #A11008); goat anti-mouse IgG (H + L) Cross-Adsorbed Secondary Antibody, Alexa Fluor 568 (1:1000, Thermo Fisher #A11004); donkey anti-goat IgG Alexa Fluor 405 (1:1000, Abcam #ab175664). Images were captured using an Olympus IX81-FV1000 microscope at ×100 magnification.

Co-Immunoprecipitation

Cells were transfected and infected as described in figure legends before being lysed in a 1-ml lysis buffer containing 50 mM HEPES-KOH (pH 7.4), 1% Triton X-100, 150 mM NaCl, 10% glycerol, and 2 mM EDTA, supplemented with Complete EDTA-free protease inhibitors (Roche, one tablet per 50 ml) and 1.5 μl of Benzonase (enzyme activity 250-300 unit/μl; Yeasen Bio #20156ES50) at 4 °C for 1 h. Lysates were incubated with anti-Flag antibody-conjugated magnetic beads (Thermo Fisher #A36797) or anti-HA antibody-conjugated magnetic beads (Thermo Fisher #88837) at 4 °C for 2 h. For enrichment of endogenous proteins, lysates were incubated with Dynabeads Protein A (Invitrogen #10002D) together with either a specific antibody or normal rabbit IgG (Millipore #12-370) as a negative control. The beads were washed three times for 10 min each with lysis buffer at 4 °C and eluted using an SDS-PAGE sample loading buffer. The eluates were analyzed by Western blots.

Proximity labeling and sample preparation for mass spectrometry (MS)

Proximity labeling was conducted according to a published protocol[51]. Briefly, the TurboID gene was cloned and fused to the N-terminus of the FOXK1, FOXF1, or FOXF1Δ200–380 gene with a linker. Unfused

TurboID served as a negative control. The primer sequences are provided in Supplementary Table 2. Plasmids pTurboID, pFOXF1-TurboID, pFOXF1Δ200–380-TurboID, and pFOXK1-TurboID were transfected into Neuro-2a cells at a concentration of 10 μg per 150-mm dish. At 42 h post-transfection, cells were infected with ICP0-null HSV-1 for 6 h at an MOI of 5, followed by treatment with 50 μM biotin for 10 min. Biotin treatment was terminated on ice, and cells were washed five times with cold PBS. Cells were lysed using RIPA buffer [50 mM Tris-HCl (pH 7.5), 150 mM NaCl, 0.1% (wt/vol) SDS, 0.5% (wt/vol) sodium deoxycholate, 1% (vol/vol) Triton X-100)] for 1 h, and the lysate was incubated with streptavidin magnetic beads (Invitrogen #65002) overnight at 4 °C. Beads were washed sequentially twice with RIPA buffer (1 ml, 2 min each), once with 1 M KCl (1 ml, 2 min), once with 0.1 M Na_2CO_3 (1 ml, ~10 s), once with 2 M urea in 10 mM Tris-HCl (pH 8.0) (1 ml, ~10 s), twice with RIPA buffer (1 ml, 2 min each), once with 200 μl of 50 mM Tris-HCl (pH 7.5), twice with 2 M urea in 50 mM Tris-HCl (pH 7.5, 200 μl, ~10 s). The final supernatant was removed, and beads were incubated with 80 μl of 2 M urea in 50 mM Tris-HCl (pH 7.5) containing 1 mM DTT and 0.4 μg trypsin at 25 °C for 1 h with vigorous shaking. The supernatant was collected and transferred to fresh tubes. Streptavidin beads were eluted twice more with 60 μl of 2 M urea in 50 mM Tris-HCl (pH 7.5), and all supernatants were combined. The released proteins were reduced by 5 mM DTT at 25 °C for 30 min and alkylated by 15 mM iodoacetamide in dark for 45 min. Additional 0.5 μg trypsin was added for overnight digestion at 25 °C. Peptides were desalted by μElute Oasis HLB plate (186001828BA, Waters) before LC-MS/MS analysis.

LC-MS/MS analysis of proximity labeling samples

Peptides (500 ng) were dissolved in 2% ACN 0.1% FA and loaded onto a reversed-phase pre-column (Acclaim PepMap 100, Thermo Scientific). Peptides were separated by a 120-min non-linear ACN gradient on a reversed-phase analytical column (Acclaim PepMap RSLC, Thermo Scientific) at a flow rate of 300 nL/min on an U3000 nanoUPLC system. Eluted peptides were analyzed by a Fusion Lumos Tribrid Orbitrap mass spectrometer (ThermoFisher Scientific). The data-independent analysis (DIA) included a full MS survey scan from 400 to 900 Th at the resolution of 240,000 FWHM (at m/z 200 Th) with automatic gain control (AGC) set to 1e6, followed by 63 MS2 spectra with isolation windows of 8 Th that covers precursors from 400-900 Th in consecutive order. Precursors co-isolated in each window were fragmented by higher-energy collision dissociation (HCD) with normalized collision energy set to 30%. All MS2 spectra were acquired with 30,000 FWHM resolution with AGC set to 2e5. All data were recorded by Xcalibur software (V4.2.28.14, Thermo Scientific). The acquired.RAW files were loaded into DIA-NN (version 1.9) for spectra-library-free search against the all SwissProt protein sequences of mouse and HSV-1 proteomes. Trypsin with up to two missed cleavages was set. Carbamidomethyl (C) was set as fixed modification. Oxidation (M) and acetyl (protein N-term) were set as variable modifications. Mass tolerance of 7 ppm and 15 ppm were set for MS and MS2 spectra, respectively. Protein level 1% FDR was set to filter the result. Potential contaminant proteins were identified by DIA-NN build-in database and were removed from subsequent analysis. For quantitative analysis, missing values were filled with a MS intensity of 1000 (noise level), and all intensity values were log2-transformed. Proteins enriched in the TurboID-labeled samples were then selected using t tests (P value < 0.05) in Excel and required a fold-change of at least 2 (corresponding to an average intergroup difference of ≥ 1 on the log2 scale).

Statistical analyses

Statistical analyses were performed using Prism version 10.0 (GraphPad Software). All measurements were taken from distinct samples. All multiple comparisons have been corrected before adjusted P values are presented. For comparisons between two groups, unpaired two-tailed t tests were used. For comparisons among three or more groups, one-way ANOVA with Dunnett's multiple comparisons tests were employed. For multi-condition group comparisons, two-way ANOVA with Sidak's multiple comparisons tests were used. To compare reactivation curves, log-rank (Mantel-Cox) tests were used. Data are expressed as mean ± SD.

Reporting summary

Further information on research design is available in the Nature Portfolio Reporting Summary linked to this article.

Data availability

Raw data for RNA-seq, ChIP-seq and ATAC-seq experiments generated in this study have been uploaded to the NCBI High-throughput Gene Expression Omnibus (GEO) repository (https://www.ncbi.nlm.nih.gov/geo/) under accession codes GSE299792, GSE285910 and GSE285909, respectively. The mass spectrometry proteomics data generated in this study have been deposited to the ProteomeXchange Consortium (https://proteomecentral.proteomexchange.org) under accession code PXD059232. The genomic sequence and the corresponding annotation files for HSV-1 strain KOS were obtained from GenBank under accession number JQ673480.1, but the files were modified to remove the terminal repeat sequences as described previously[21]. Mouse (mm10) genomic sequence and annotation files were downloaded from the UCSC Genome Browser (https://genome.ucsc. edu/cgi-bin/hgGateway?db=mm10). *Fox* gene expression data were obtained from the Protein Atlas database (https://www.proteinatlas.org/). Source data are provided with this paper.

Code availability

Multiple alignment of FOX protein DBD sequences was performed using GENEDOC software. The FOXC2 DBD-DNA complex structure was obtained from the PDB (6AKO) and visualized in PyMOL. STRING network analysis diagrams were generated using the STRING database (https://cn.string-db.org/). KEGG analysis was conducted using DAVID Bioinformatics Resources (https://davidbioinformatics.nih.gov/tools.jsp). The mechanistic model (Fig. 7i) was created using the BioGDP platform (https://biogdp.com).

References

1. Knipe, D. M., Heldwein, E. F., Mohr, I. J. & Sodroski, C. N. Herpes simplex viruses. In *Fields Virology* Vol. 1 (eds. Howley, P. M. et al.) 235–296 (Lippincott Williams & Wilkins, 2021).
2. Fu, H. & Pan, D. Mechanisms of HSV gene regulation during latency and reactivation. *Virology* **602**, 110324 (2025).
3. Knipe, D. M. & Cliffe, A. Chromatin control of herpes simplex virus lytic and latent infection. *Nat. Rev. Microbiol.* **6**, 211–221 (2008).
4. Kwiatkowski, D. L., Thompson, H. W. & Bloom, D. C. The polycomb group protein Bmi1 binds to the herpes simplex virus 1 latent genome and maintains repressive histone marks during latency. *J. Virol.* **83**, 8173–8181 (2009).
5. Wang, Q. Y. et al. Herpesviral latency-associated transcript gene promotes assembly of heterochromatin on viral lytic-gene promoters in latent infection. *Proc. Natl. Acad. Sci. USA* **102**, 16055–16059 (2005).
6. Cliffe, A. R., Garber, D. A. & Knipe, D. M. Transcription of the herpes simplex virus latency-associated transcript promotes the formation of facultative heterochromatin on lytic promoters. *J. Virol.* **83**, 8182–8190 (2009).
7. Liang, Y. et al. Targeting the JMJD2 histone demethylases to epigenetically control herpesvirus infection and reactivation from latency. *Sci. Transl. Med.* **5**, 167ra165 (2013).
8. Liang, Y., Vogel, J. L., Narayanan, A., Peng, H. & Kristie, T. M. Inhibition of the histone demethylase LSD1 blocks alpha-herpesvirus lytic replication and reactivation from latency. *Nat. Med.* **15**, 1312–1317 (2009).

9. Messer, H. G., Jacobs, D., Dhummakupt, A. & Bloom, D. C. Inhibition of H3K27me3-specific histone demethylases JMJD3 and UTX blocks reactivation of herpes simplex virus 1 in trigeminal ganglion neurons. *J. Virol.* **89**, 3417–3420 (2015).
10. Hill, J. M. et al. Inhibition of LSD1 reduces herpesvirus infection, shedding, and recurrence by promoting epigenetic suppression of viral genomes. *Sci. Transl. Med.* **6**, 265ra169 (2014).
11. Camarena, V. et al. Nature and duration of growth factor signaling through receptor tyrosine kinases regulates HSV-1 latency in neurons. *Cell Host microbe* **8**, 320–330 (2010).
12. Kim, J. Y., Mandarino, A., Chao, M. V., Mohr, I. & Wilson, A. C. Transient reversal of episome silencing precedes VP16-dependent transcription during reactivation of latent HSV-1 in neurons. *PLoS Pathog.* **8**, e1002540 (2012).
13. Kobayashi, M., Wilson, A. C., Chao, M. V. & Mohr, I. Control of viral latency in neurons by axonal mTOR signaling and the 4E-BP translation repressor. *Genes Dev.* **26**, 1527–1532 (2012).
14. Hu, H. L. et al. TOP2β-dependent nuclear DNA damage shapes extracellular growth factor responses via dynamic akt phosphorylation to control virus latency. *Mol. Cell* **74**, 466–480.e464 (2019).
15. Suzich, J. B. et al. PML-NB-dependent type I interferon memory results in a restricted form of HSV latency. *EMBO Rep.* **22**, e52547 (2021).
16. Cohen, C. et al. Promyelocytic leukemia (PML) nuclear bodies (NBs) induce latent/quiescent HSV-1 genomes chromatinization through a PML NB/Histone H3.3/H3.3 chaperone axis. *PLoS Pathog.* **14**, e1007313 (2018).
17. Cabral, J. M., Cushman, C. H., Sodroski, C. N. & Knipe, D. M. ATRX limits the accessibility of histone H3-occupied HSV genomes during lytic infection. *PLoS Pathog.* **17**, e1009567 (2021).
18. Aggarwal, A. et al. Ultrastructural visualization of individual tegument protein dissociation during entry of herpes simplex virus 1 into human and rat dorsal root ganglion neurons. *J. Virol.* **86**, 6123–6137 (2012).
19. Hafezi, W. et al. Entry of herpes simplex virus type 1 (HSV-1) into the distal axons of trigeminal neurons favors the onset of nonproductive, silent infection. *PLoS Pathog.* **8**, e1002679 (2012).
20. Pan, D. et al. A neuron-specific host microRNA targets herpes simplex virus-1 ICP0 expression and promotes latency. *Cell Host Microbe* **15**, 446–456 (2014).
21. Sun, B. et al. Regulation of host and virus genes by neuronal miR-138 favours herpes simplex virus 1 latency. *Nat. Microbiol.* **6**, 682–696 (2021).
22. Chen, S. et al. Neuronal miR-138 represses HSV-2 lytic infection by regulating viral and host genes with mechanistic differences from HSV-1. *J. Virol.* **96**, e0034922 (2022).
23. Deng, Y. et al. Neuronal miR-9 promotes HSV-1 epigenetic silencing and latency by repressing Oct-1 and Onecut family genes. *Nat. Commun.* **15**, 1991 (2024).
24. Cliffe, A. R. et al. Neuronal stress pathway mediating a histone methyl/phospho switch is required for herpes simplex virus reactivation. *Cell Host Microbe* **18**, 649–658 (2015).
25. Whitford, A. L. et al. Ex vivo herpes simplex virus reactivation involves a dual leucine zipper kinase-dependent wave of lytic gene expression that is independent of histone demethylase activity and viral genome synthesis. *J. Virol.* **96**, e0047522 (2022).
26. Harrison, K. S. et al. Impaired glucocorticoid receptor function attenuates herpes simplex virus 1 production during explant-induced reactivation from latency in female mice. *J. Virol.* **97**, e0130523 (2023).
27. Ostler, J. B., Thunuguntla, P., Hendrickson, B. Y. & Jones, C. Transactivation of herpes simplex virus 1 (HSV-1) infected cell protein 4 enhancer by glucocorticoid receptor and stress-induced transcription factors requires overlapping Krüppel-like transcription factor 4/Sp1 binding sites. *J. Virol.* **95**, e01776-20 (2021).
28. Jackson, B. C., Carpenter, C., Nebert, D. W. & Vasiliou, V. Update of human and mouse forkhead box (FOX) gene families. *Hum. Genomics* **4**, 345–352 (2010).
29. Hannenhalli, S. & Kaestner, K. H. The evolution of Fox genes and their role in development and disease. *Nat. Rev. Genet.* **10**, 233–240 (2009).
30. Lam, E. W., Brosens, J. J., Gomes, A. R. & Koo, C. Y. Forkhead box proteins: tuning forks for transcriptional harmony. *Nat. Rev. Cancer* **13**, 482–495 (2013).
31. Adams, E. J. et al. FOXA1 mutations alter pioneering activity, differentiation and prostate cancer phenotypes. *Nature* **571**, 408–412 (2019).
32. Herman, L., Todeschini, A. L. & Veitia, R. A. Forkhead transcription factors in health and disease. *Trends Genet.* **37**, 460–475 (2021).
33. Cirillo, L. A. et al. Opening of compacted chromatin by early developmental transcription factors HNF3 (FoxA) and GATA-4. *Mol. cell* **9**, 279–289 (2002).
34. Iwafuchi-Doi, M. et al. The pioneer transcription factor FoxA maintains an accessible nucleosome configuration at enhancers for tissue-specific gene activation. *Mol. Cell* **62**, 79–91 (2016).
35. Palmer, M. et al. Conserved linear motif within the immediate early protein ORF45 promotes its engagement with KSHV lytic cycle-promoting forkhead transcription factors, FOXK1 and FOXK2. *J. Virol.* **98**, e0088624 (2024).
36. Chen, Q. et al. FoxK1 and FoxK2 cooperate with ORF45 to promote late lytic replication of Kaposi's sarcoma-associated herpesvirus. *J. Virol.* **98**, e0077924 (2024).
37. Lan, J. et al. Targeting FoxO proteins induces lytic reactivation of KSHV for treating herpesviral primary effusion lymphoma. *PLoS Pathog.* **19**, e1011581 (2023).
38. Hale, A. E. et al. FOXO transcription factors activate alternative major immediate early promoters to induce human cytomegalovirus reactivation. *Proc. Natl. Acad. Sci. USA* **117**, 18764–18770 (2020).
39. Zhang, H., Domma, A. J., Goodrum, F. D., Moorman, N. J. & Kamil, J. P. The Akt forkhead box O transcription factor axis regulates human cytomegalovirus replication. *mBio* **13**, e0104222 (2022).
40. Rodríguez, M. C., Dybas, J. M., Hughes, J., Weitzman, M. D. & Boutell, C. The HSV-1 ubiquitin ligase ICP0: modifying the cellular proteome to promote infection. *Virus Res.* **285**, 198015 (2020).
41. Cai, W. Z. & Schaffer, P. A. Herpes simplex virus type 1 ICP0 plays a critical role in the de novo synthesis of infectious virus following transfection of viral DNA. *J. Virol.* **63**, 4579–4589 (1989).
42. Oh, H. S. et al. Validation of human sensory neurons derived from inducible pluripotent stem cells as a model for latent infection and reactivation by herpes simplex virus 1. *mBio* **16**, e01871-25 (2025).
43. Berra, L. V., Armocida, D., Pesce, A., Di Rita, A. & Santoro, A. Herpes simplex reactivation after surgical treatment of trigeminal neuralgia: a retrospective cohort study. *World Neurosurg.* **127**, e16–e21 (2019).
44. Sawtell, N. M. & Thompson, R. L. Rapid in vivo reactivation of herpes simplex virus in latently infected murine ganglionic neurons after transient hyperthermia. *J. Virol.* **66**, 2150–2156 (1992).
45. Zhou, X. et al. Deletion of PIK3C3/Vps34 in sensory neurons causes rapid neurodegeneration by disrupting the endosomal but not the autophagic pathway. *Proc. Natl. Acad. Sci. USA* **107**, 9424–9429 (2010).
46. Ran, L. et al. FOXF1 defines the core-regulatory circuitry in gastrointestinal stromal tumor. *Cancer Discov.* **8**, 234–251 (2018).
47. Chen, X. et al. Structural basis for DNA recognition by FOXC2. *Nucleic Acids Res.* **47**, 3752–3764 (2019).
48. Catez, F. et al. HSV-1 genome subnuclear positioning and associations with host-cell PML-NBs and centromeres regulate LAT locus transcription during latency in neurons. *PLoS Pathog.* **8**, e1002852 (2012).

49. Alandijany, T. et al. Distinct temporal roles for the promyelocytic leukaemia (PML) protein in the sequential regulation of intracellular host immunity to HSV-1 infection. *PLoS Pathog.* **14**, e1006769 (2018).
50. Lukashchuk, V. & Everett, R. D. Regulation of ICP0-null mutant herpes simplex virus type 1 infection by ND10 components ATRX and hDaxx. *J. Virol.* **84**, 4026–4040 (2010).
51. Cho, K. F. et al. Proximity labeling in mammalian cells with TurboID and split-TurboID. *Nat. Protoc.* **15**, 3971–3999 (2020).
52. Arany, Z., Sellers, W. R., Livingston, D. M. & Eckner, R. E1A-associated p300 and CREB-associated CBP belong to a conserved family of coactivators. *Cell* **77**, 799–800 (1994).
53. Lasko, L. M. et al. Discovery of a selective catalytic p300/CBP inhibitor that targets lineage-specific tumours. *Nature* **550**, 128–132 (2017).
54. Laherty, C. D. et al. Histone deacetylases associated with the mSin3 corepressor mediate mad transcriptional repression. *Cell* **89**, 349–356 (1997).
55. Bertke, A. S. et al. A5-positive primary sensory neurons are non-permissive for productive infection with herpes simplex virus 1 in vitro. *J. Virol.* **85**, 6669–6677 (2011).
56. Shi, X. & Garry, D. J. Sin3 interacts with Foxk1 and regulates myogenic progenitors. *Mol. Cell Biochem.* **366**, 251–258 (2012).
57. Bowman, C. J., Ayer, D. E. & Dynlacht, B. D. Foxk proteins repress the initiation of starvation-induced atrophy and autophagy programs. *Nat. Cell Biol.* **16**, 1202–1214 (2014).
58. Caravaca, J. M. et al. Bookmarking by specific and nonspecific binding of FoxA1 pioneer factor to mitotic chromosomes. *Genes Dev.* **27**, 251–260 (2013).
59. Sekiya, T., Muthurajan, U. M., Luger, K., Tulin, A. V. & Zaret, K. S. Nucleosome-binding affinity as a primary determinant of the nuclear mobility of the pioneer transcription factor FoxA. *Genes Dev.* **23**, 804–809 (2009).
60. Soufi, A. et al. Pioneer transcription factors target partial DNA motifs on nucleosomes to initiate reprogramming. *Cell* **161**, 555–568 (2015).
61. Iwafuchi, M. et al. Gene network transitions in embryos depend upon interactions between a pioneer transcription factor and core histones. *Nat. Genet* **52**, 418–427 (2020).
62. Deshmane, S. L. & Fraser, N. W. During latency, herpes simplex virus type 1 DNA is associated with nucleosomes in a chromatin structure. *J. Virol.* **63**, 943–947 (1989).
63. Barral, A. & Zaret, K. S. Pioneer factors: roles and their regulation in development. *Trends Genet.* **40**, 134–148 (2024).
64. Millán-Zambrano, G., Burton, A., Bannister, A. J. & Schneider, R. Histone post-translational modifications - cause and consequence of genome function. *Nat. Rev. Genet.* **23**, 563–580 (2022).
65. Blackwood, E. M. & Eisenman, R. N. Max: a helix-loop-helix zipper protein that forms a sequence-specific DNA-binding complex with Myc. *Science* **251**, 1211–1217 (1991).
66. Katzenell, S., Cabrera, J. R., North, B. J. & Leib, D. A. Isolation, purification, and culture of primary murine sensory neurons. *Methods Mol. Biol.* **1656**, 229–251 (2017).
67. Ng, A. H. M. et al. A comprehensive library of human transcription factors for cell fate engineering. *Nat. Biotechnol.* **39**, 510–519 (2021).
68. Yan, K. et al. The carboxyl terminus of tegument protein pUL21 contributes to pseudorabies virus neuroinvasion. *J. Virol.* **93**, https://doi.org/10.1128/jvi.02052-18 (2019).
69. Liu, Z. F., Brum, M. C., Doster, A., Jones, C. & Chowdhury, S. I. A bovine herpesvirus type 1 mutant virus specifying a carboxyl-terminal truncation of glycoprotein E is defective in anterograde neuronal transport in rabbits and calves. *J. Virol.* **82**, 7432–7442 (2008).
70. Visalli, M. A., House, B. L., Selariu, A., Zhu, H. & Visalli, R. J. The varicella-zoster virus portal protein is essential for cleavage and packaging of viral DNA. *J. Virol.* **88**, 7973–7986 (2014).
71. Yang, X. et al. Host MOV10 is induced to restrict herpes simplex virus 1 lytic infection by promoting type I interferon response. *PLoS Pathog.* **18**, e1010301 (2022).
72. Dobin, A. et al. STAR: ultrafast universal RNA-seq aligner. *Bioinformatics* **29**, 15–21 (2013).
73. Patro, R., Duggal, G., Love, M. I., Irizarry, R. A. & Kingsford, C. Salmon provides fast and bias-aware quantification of transcript expression. *Nat. Methods* **14**, 417–419 (2017).
74. Soneson, C., Love, M. I. & Robinson, M. D. Differential analyses for RNA-seq: transcript-level estimates improve gene-level inferences. *F1000Research* **4**, 1521 (2015).
75. Gu, Z., Eils, R. & Schlesner, M. Complex heatmaps reveal patterns and correlations in multidimensional genomic data. *Bioinformatics* **32**, 2847–2849 (2016).
76. Rosato, P. C. et al. Neuronal IFN signaling is dispensable for the establishment of HSV-1 latency. *Virology* **497**, 323–327 (2016).

Acknowledgements

We thank Liang Wang of Zhejiang University School of Medicine for providing Advillin-Cre mice, George Church of Harvard Medical School for providing iNGN3 iPSCs, Zhengfei Liu of Huazhong Agricultural University for providing PRV and BoHV-1, Liqian Zhu of Hebei University for providing MDBK cells, Yaowei Huang of Zhejiang University for providing PK15 cells and Hua Zhu of Rutgers University for providing VZV BAC DNA. We thank Qianbing Zhao at the Core Facility of Zhejiang University School of Medicine for expertise and instrument availability. We thank Jiaqi Li for assistance in high-throughput sequencing analysis. This work was supported by the National Key R & D Program of China (2023YFC2306702 and 2024YFA1306602 to D.P.), National Natural Science Foundation of China (82272322 to D.P.), Natural Science Foundation of Zhejiang Province (LZ23H190001 to D.P.), National Institute of Allergy and Infectious Diseases (5P01AI098681 to D.C. and D.K.; P01AI177687 to S.J.), NHLBI/NIH (K08HL157725 to P.S.) and American Heart Association (Career Development Award to P.S.), and an NIH Director's Pioneer Award (DP2AI171139 to S.J.).

Author contributions

D.P. conceived and supervised the study and wrote the first draft of the article. D.P. also performed mouse neuronal culture experiments and contributed to ChIP-qPCR experiments. Y.X. performed molecular cloning, transfection and infection experiments in cell culture, ChIP-qPCR, ChIP-seq and ATAC-seq experiments, proximity labeling, immunoprecipitation, immunofluorescence, animal experiments, and data analysis and maintenance. X.Y. and J.Z. performed some cloning, cell culture and animal experiments. X.Y. also constructed N2A-FOXK1KO cells. F.H., Y.D. and Q.W. contributed to cloning and cell culture experiments. H.F. contributed to mouse neuronal culture experiments. H.S.O. and B.D. performed experiments on iPSC-derived human neurons. S.C. contributed to the maintenance of genetically modified mice. Z.S. performed mass spectrometry analysis. B.D., J.M.P. and P.S. designed and performed RNA-seq studies of iPSC-derived human neurons and Y.Y.Y. and S.J. analyzed the data. D.M.K. and D.M.C. supervised the experiments related to iPSC-derived neurons. All authors reviewed and approved the manuscript.

Competing interests

S.J. is a co-founder of Elucidate Bio Inc., and serves on its Board of Directors and Scientific Advisory Board, and has received research support from Roche and Novartis. The authors declare no competing interests.

Additional information

Supplementary information The online version contains supplementary material available at https://doi.org/10.1038/s41467-026-68915-1.

Correspondence and requests for materials should be addressed to Dongli Pan.

Peer review information *Nature Communications* thanks Adam Whisnant, Lucas Wilken, and the other, anonymous, reviewer for their contribution to the peer review of this work. A peer review file is available.

Reprints and permissions information is available at http://www.nature.com/reprints

Publisher's note Springer Nature remains neutral with regard to jurisdictional claims in published maps and institutional affiliations.

Open Access This article is licensed under a Creative Commons Attribution-NonCommercial-NoDerivatives 4.0 International License, which permits any non-commercial use, sharing, distribution and reproduction in any medium or format, as long as you give appropriate credit to the original author(s) and the source, provide a link to the Creative Commons licence, and indicate if you modified the licensed material. You do not have permission under this licence to share adapted material derived from this article or parts of it. The images or other third party material in this article are included in the article's Creative Commons licence, unless indicated otherwise in a credit line to the material. If material is not included in the article's Creative Commons licence and your intended use is not permitted by statutory regulation or exceeds the permitted use, you will need to obtain permission directly from the copyright holder. To view a copy of this licence, visit http://creativecommons.org/licenses/by-nc-nd/4.0/.

© The Author(s) 2026